Lithium processing in stars
Diagnosis for stellar structure and evolution

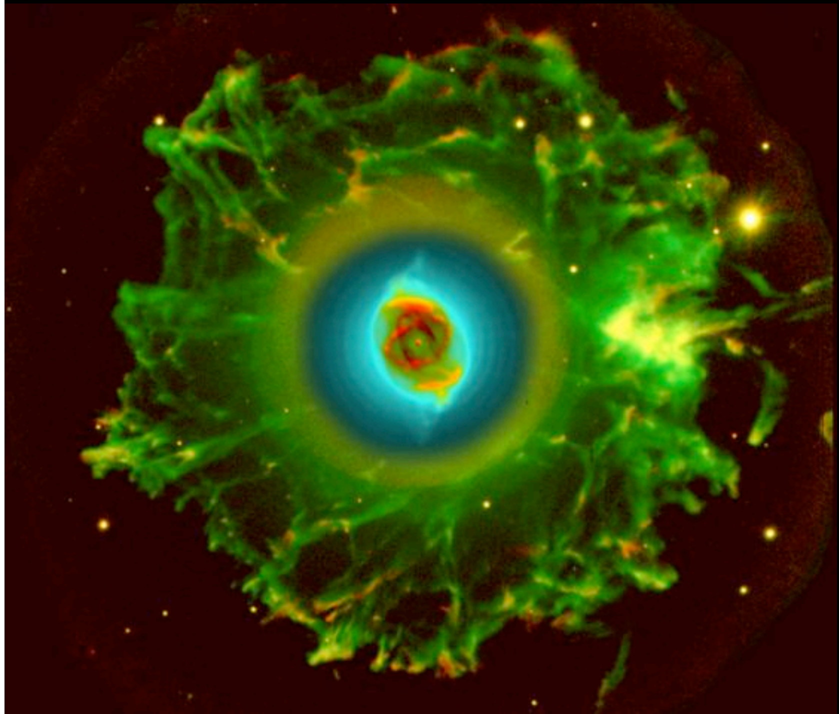

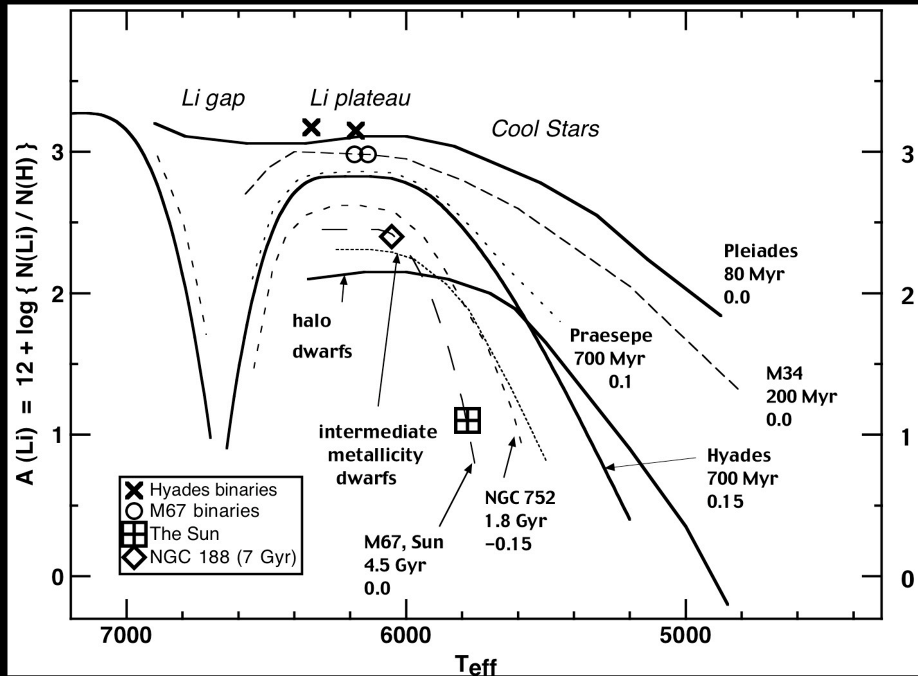

Corinne Charbonnel

Geneva Observatory (Switzerland) & CNRS (France)

S.Talon, T.Decressin, P.Eggenberger, S.Mathis

Montreal (Canada), Geneva (Switzerland), CEA (France)

UNIVERSITÉ DE GENÈVE
FACULTÉ DES SCIENCES

CNRS
CENTRE NATIONAL DE LA RECHERCHE SCIENTIFIQUE

LITHIUM IN THE COSMOS

Abundance tomography in low-mass stars

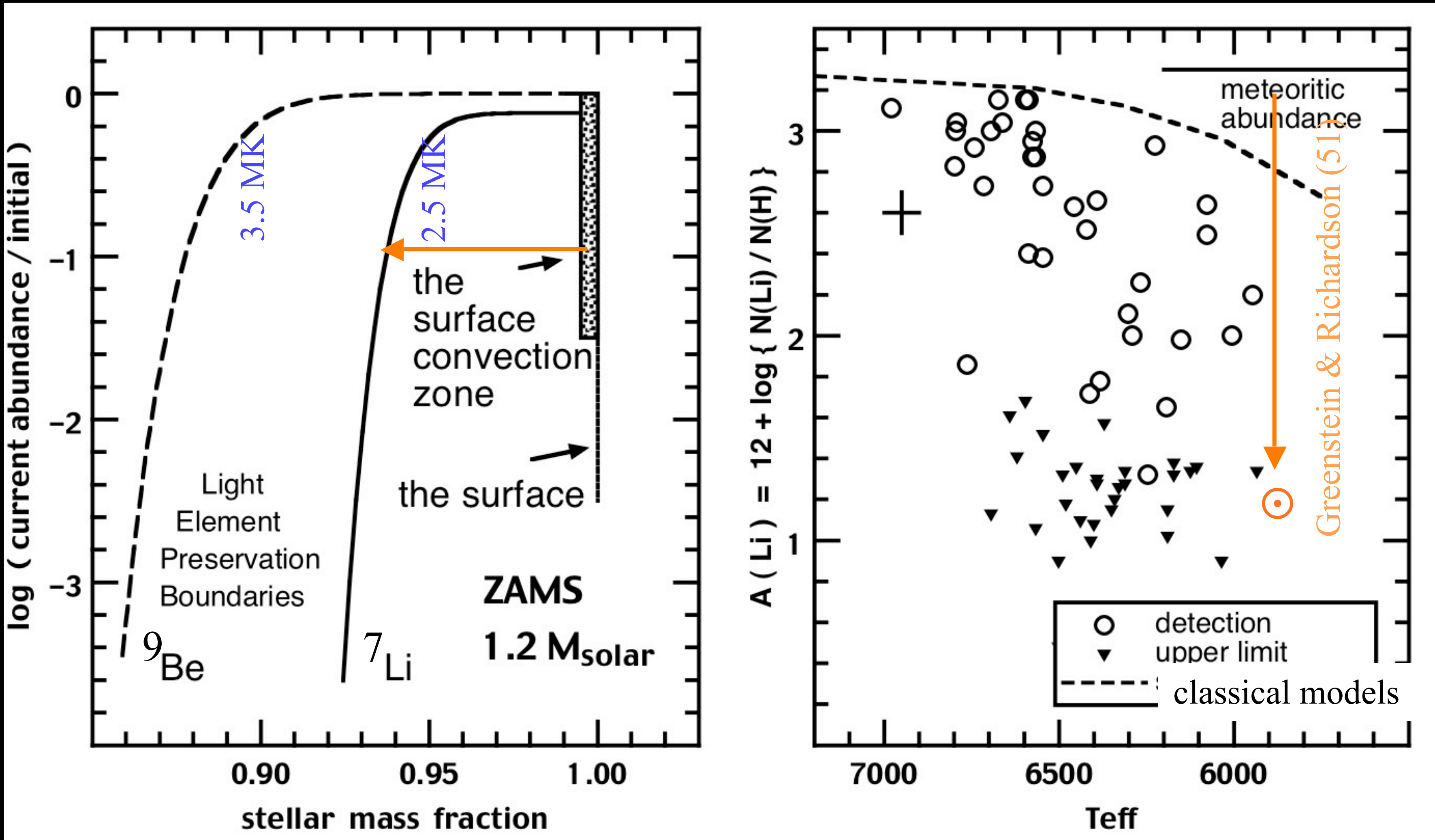

Data in field stars
by Boesgaard & Tripicco (86b)

Fig. from Deliyannis, Pinsonneault & Charbonnel (00)

The lithium dip

First observed in the Hyades (Wallerstein, Herbig & Conti 65; Boesgaard & Tripicco 86a)

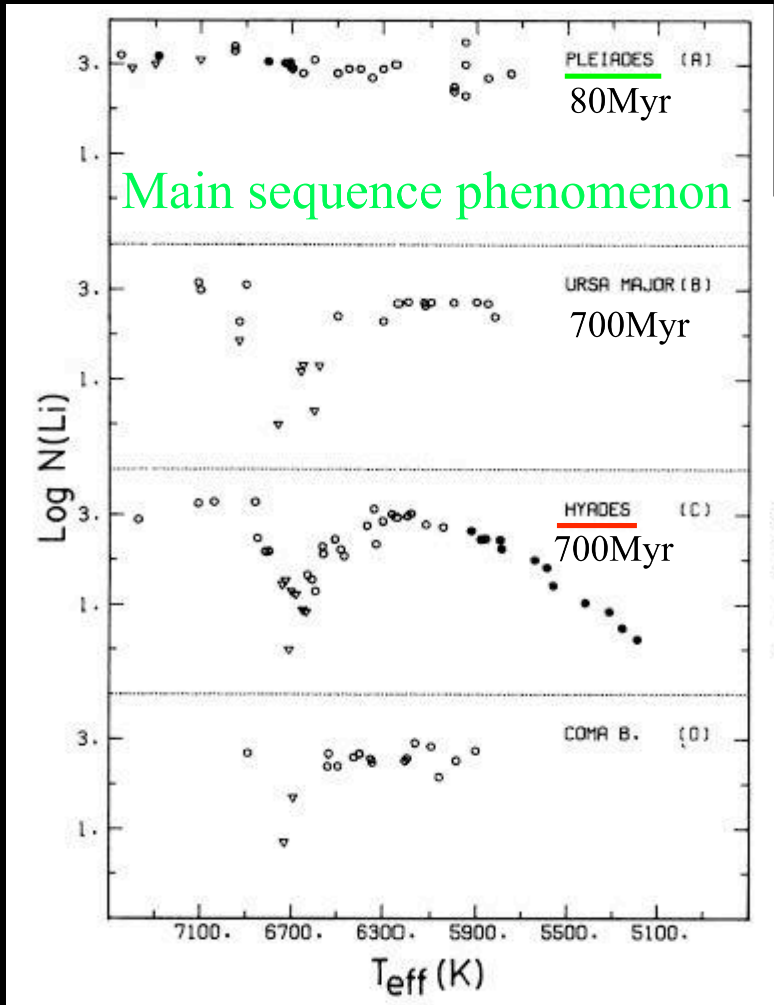

Observed in
all open clusters older than ~ 200 Myr
and in field stars (Balachandran 95)

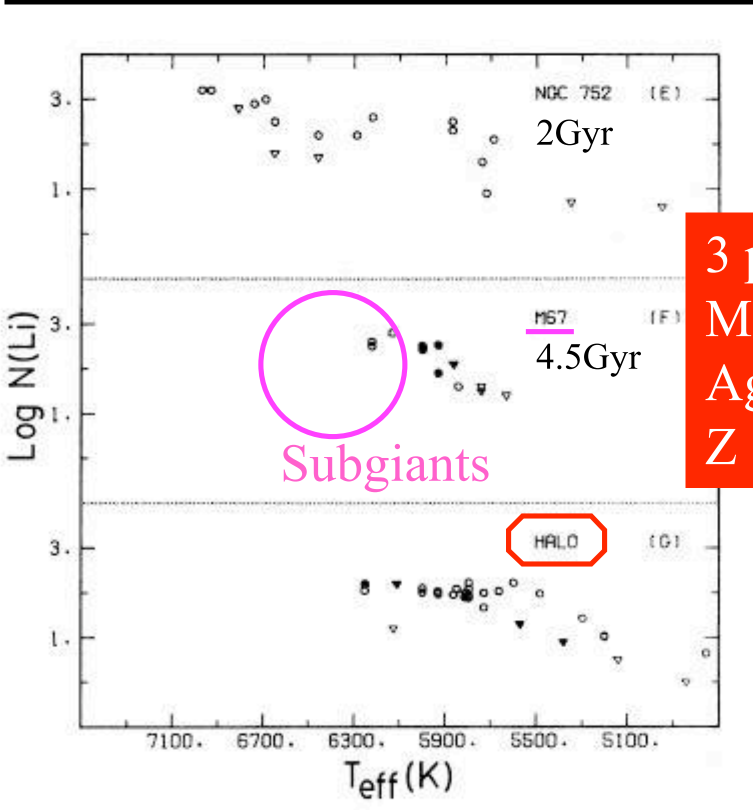

3 parameters:
M_* (~Teff)
Age
Z

Fig. from Charbonneau & Michaud (88)

The lithium dip - Atomic diffusion

New radiative force calculations (Richer et al. 99)

→ **Mloss ~ 10^{-15} $M_\odot$ yr $^{-1}$**

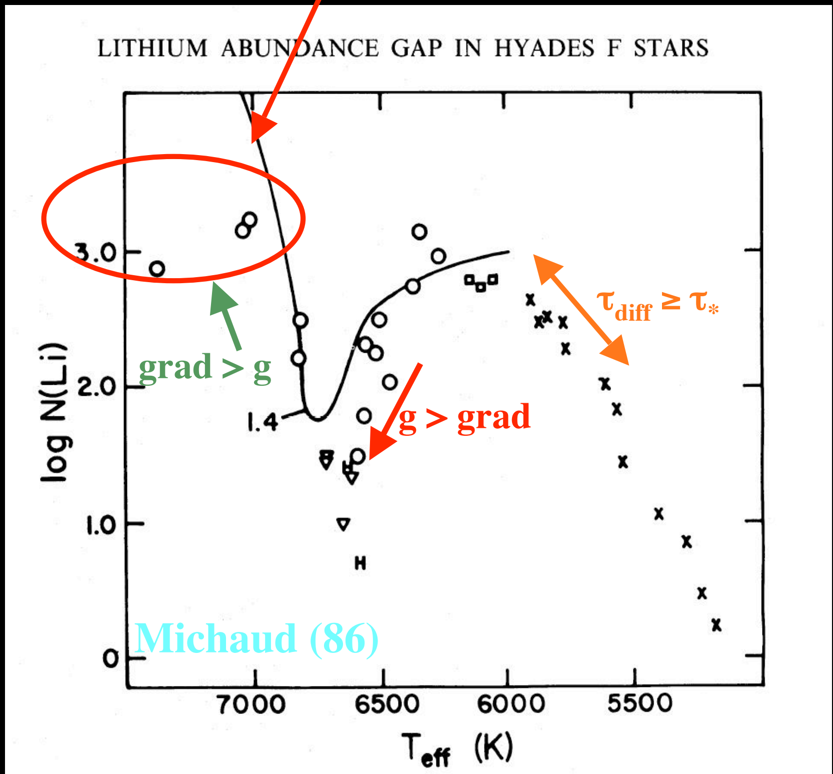

Diffusion becomes increasingly efficient with decreasing density below the CE, i.e., with increasing Teff

Michaud (86) → Michaud et al. (00)

+ Gravit. settling, thermal diffusion (↓) & radiative acceleration (↑)
+ Calculated entirely from first principles

The lithium dip - Atomic diffusion

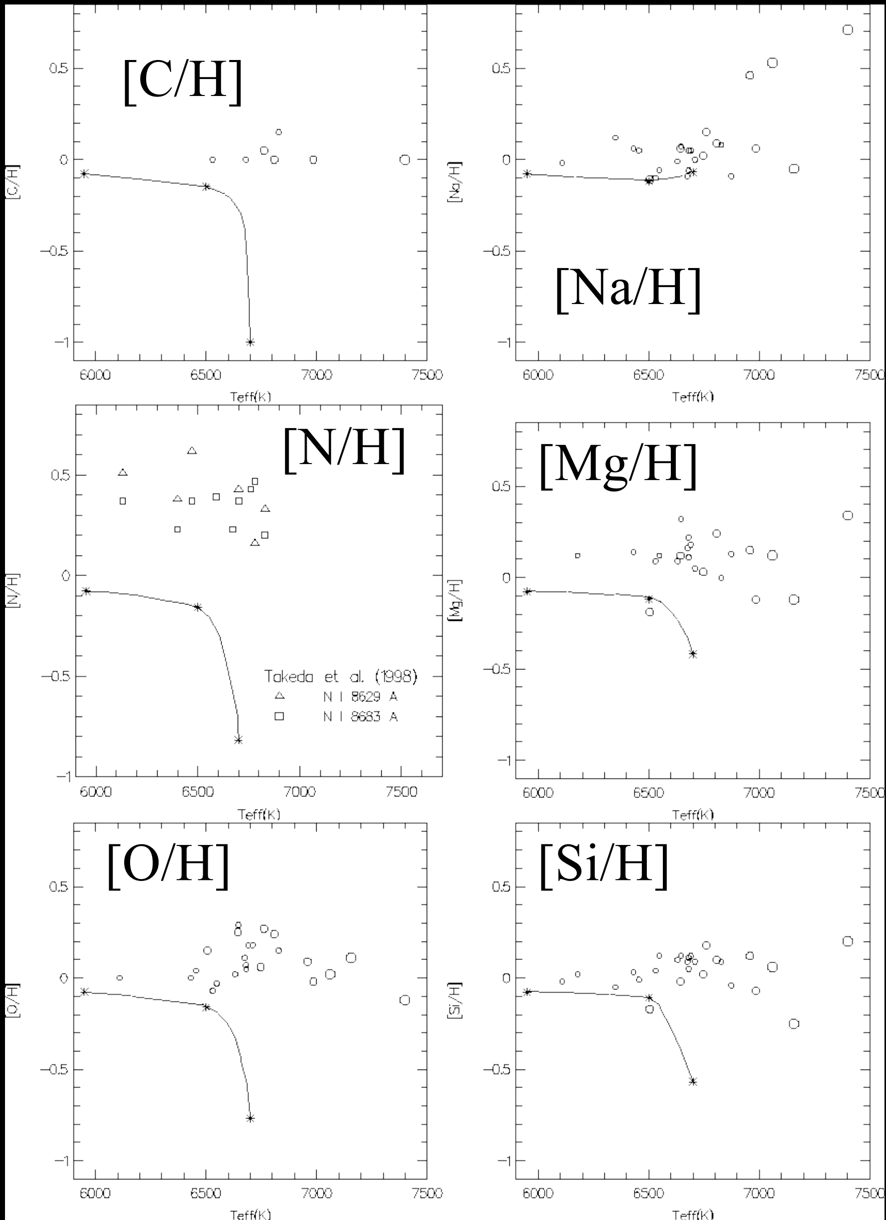

Problems :

✓ Heavy elements are also expected to settle down in Li-deficient stars

→ Incompatible with the observational data across the dip

Fig. and data in the Hyades from Varenne & Monier (99)
Predictions by Turcotte et al. (98)

See also Gebran, Monier & Richard (08) for the Pleiades and ComaB

The lithium dip - Atomic diffusion

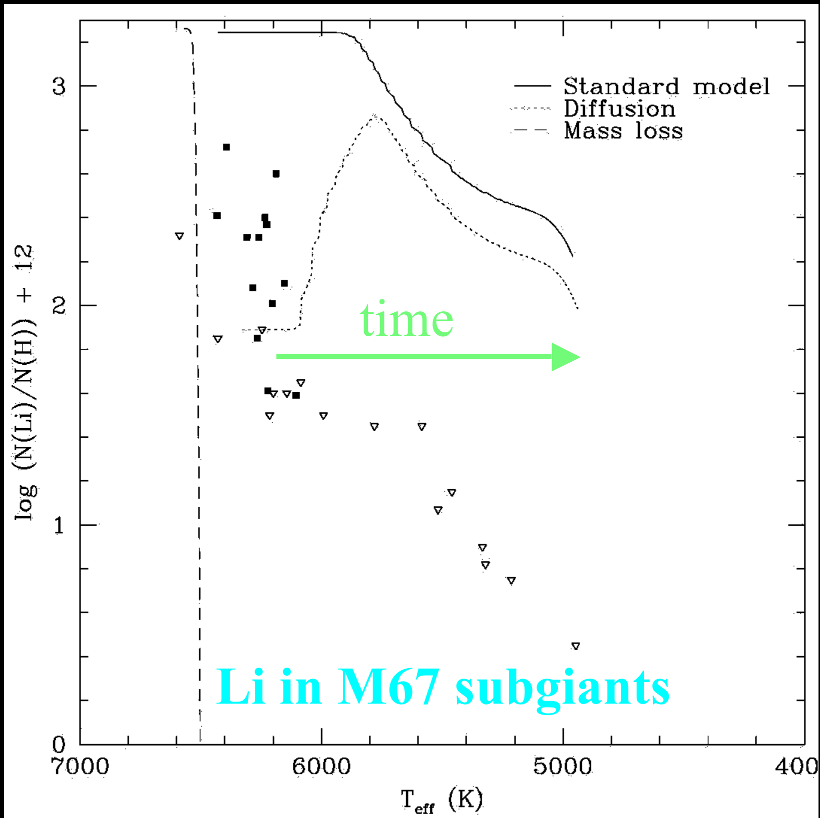

Deliyannis et al. (97)
See also Pilachowski et al. (88)
& Balachandran (95)

Problems :

✓ Li is not destroyed, it just settles out of the convective envelope

→ Incompatible with the Li data in the Herzsprung gap (field and open cluster subgiants)

→ Strongly favours explanations relying on nuclear destruction of Li

Atomic diffusion is *not the only* process responsible for the Li dip in open clusters

The lithium dip - Rotation

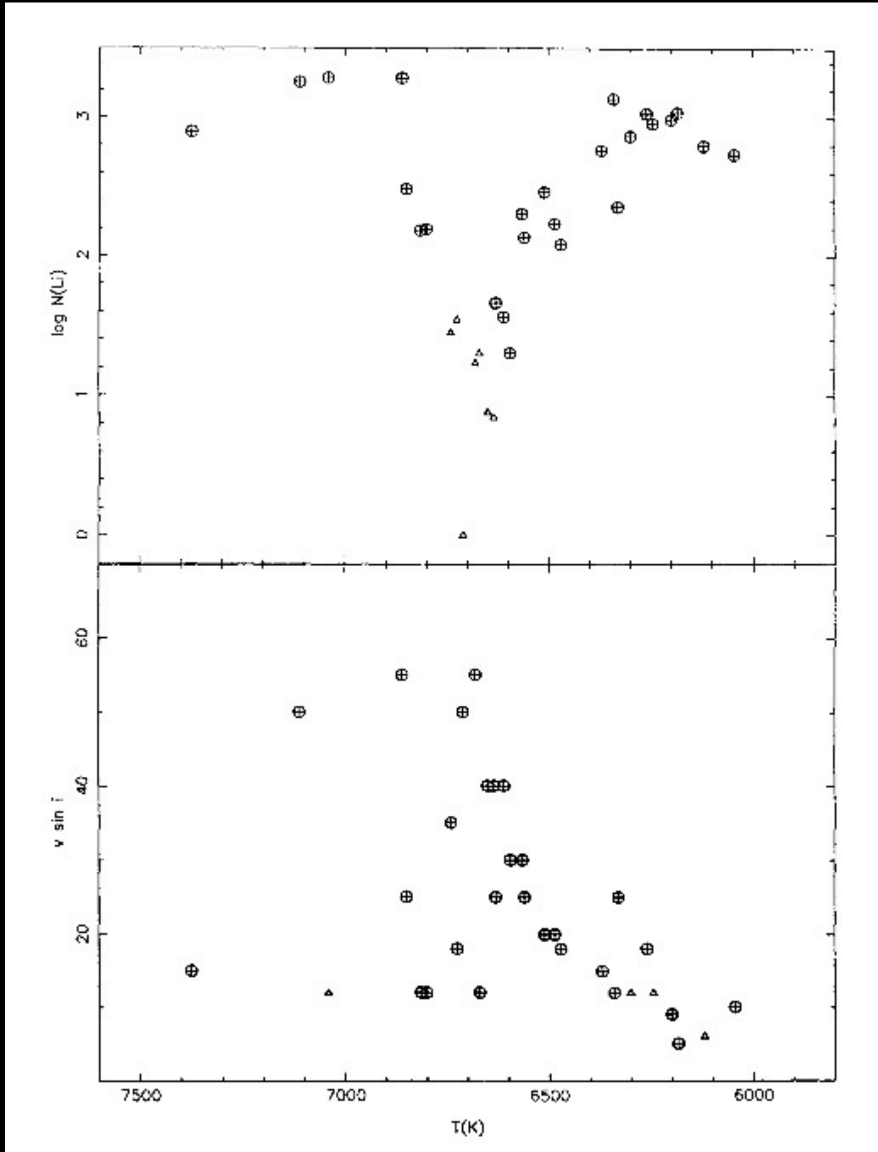

Boesgaard (87)

The lithium dip : A pivotal Teff
for stellar structure and rotational history

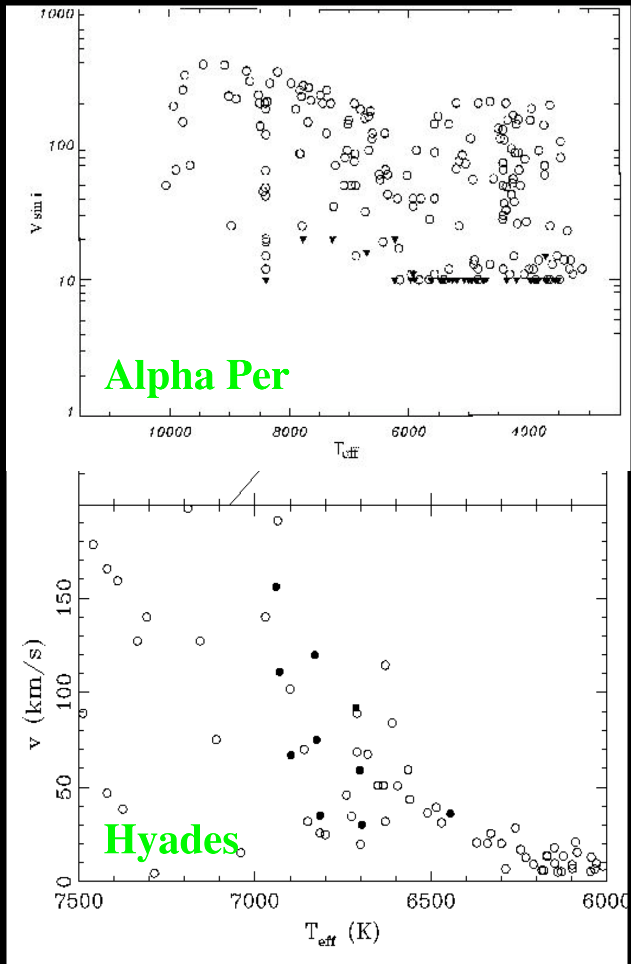

Physical processes for the evolution of the surface velocity are different, or operate on different timescales on each side of the dip

The lithium dip : A pivotal Teff for stellar structure and rotational history

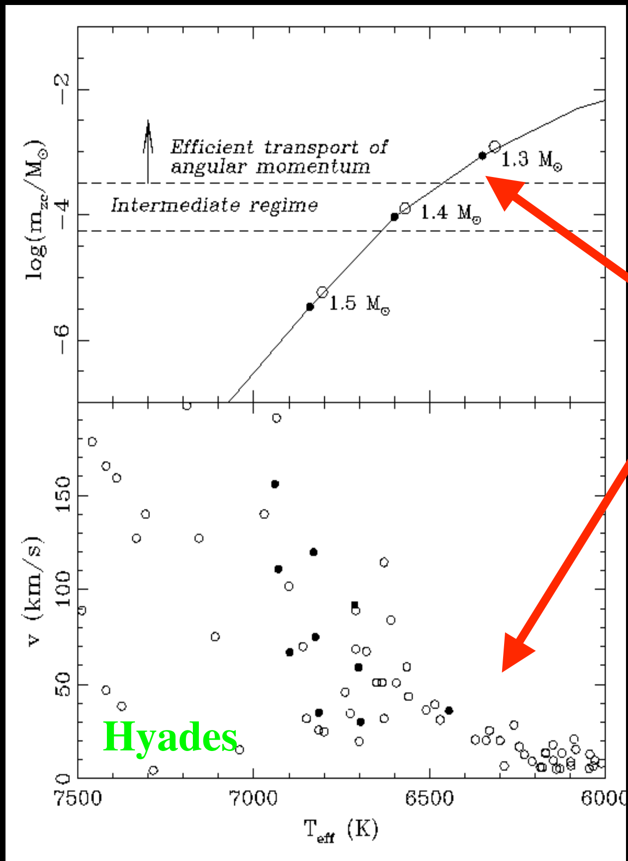

Deep enough surface convective region
to sustain a dynamo
and to produce a surface magnetic field
that is then responsible for efficient braking

The lithium dip : A pivotal Teff for stellar structure and rotational history

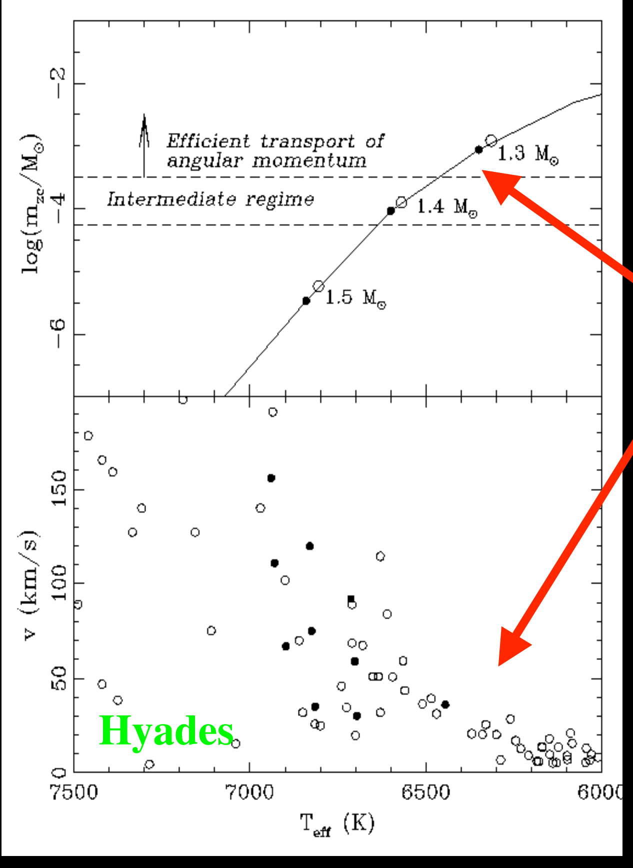

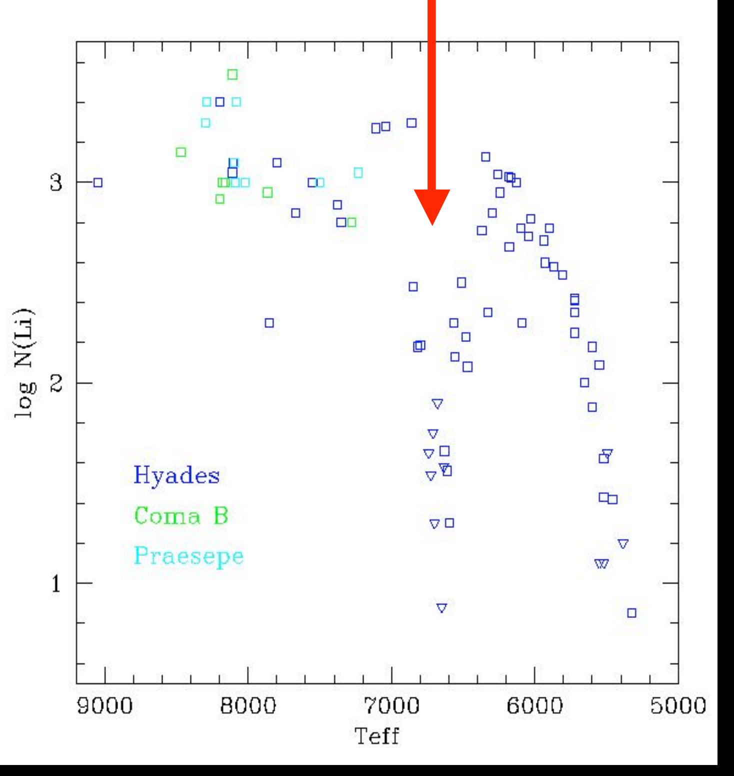

Transport of angular momentum (advection + turbulence)

$$\frac{\mathrm{d}}{\mathrm{d}t}\left[r^2\Omega\right] = \frac{1}{5r^2}\frac{\partial}{\partial r}\left[\, r^4\Omega U_2\right] + \frac{1}{r^2}\frac{\partial}{\partial r}\quad {}_{\mathrm{v}}r^4\frac{\partial\Omega}{\partial r}$$

Contraction or expansion — Advection (MC) — Diffusion (shear)

Thermal unbalance $\Longrightarrow$ Meridional circulation

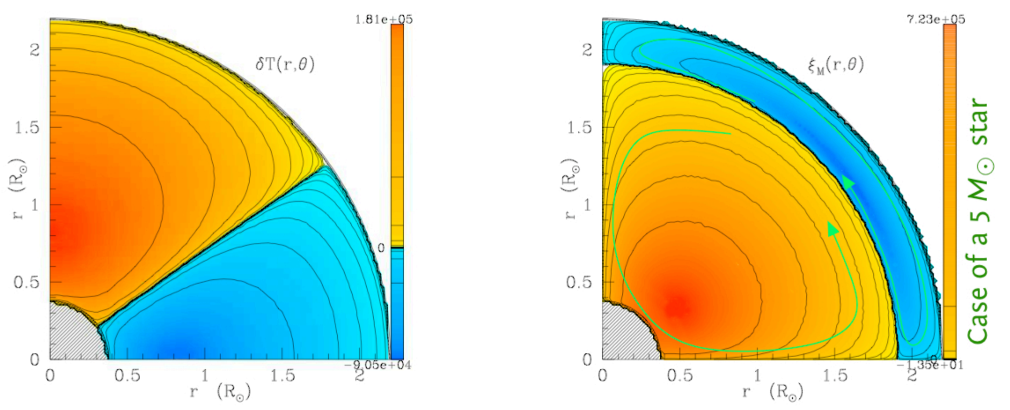

Ω-gradient $\Longrightarrow$ Shear turbulence

Transport of chemicals

$$\rho\frac{\mathrm{d}Y_i}{\mathrm{d}t} = \underbrace{\rho\frac{\mathrm{d}Y_i}{\mathrm{d}t}}_{\text{nuclear}} + \underbrace{\frac{1}{r^2}\frac{\partial}{\partial r}\left[r^2\rho\left(D_{\mathrm{eff}} + D_{\mathrm{v}}\right)\frac{\partial Y_i}{\partial r}\right]}_{\text{diffusion by MC and shear}}$$

Zahn (1992), Chaboyer & Zahn (1992), Talon & Zahn (1997), Maeder & Zahn (1998), Mathis & Zahn (2004), Decressin et al. (2009)

Rotation-induced mixing :
The hot side of the lithium dip

Teff ≥ 6900 K : Very shallow surface convective zone
Uneficient magnetic generation via a dynamo process
Not slowed down by a magnetic torque

Angular momentum loss
drives circulation and depletes Li

Regime with no net angular momentum flux
The weak mixing counterbalances atomic diffusion

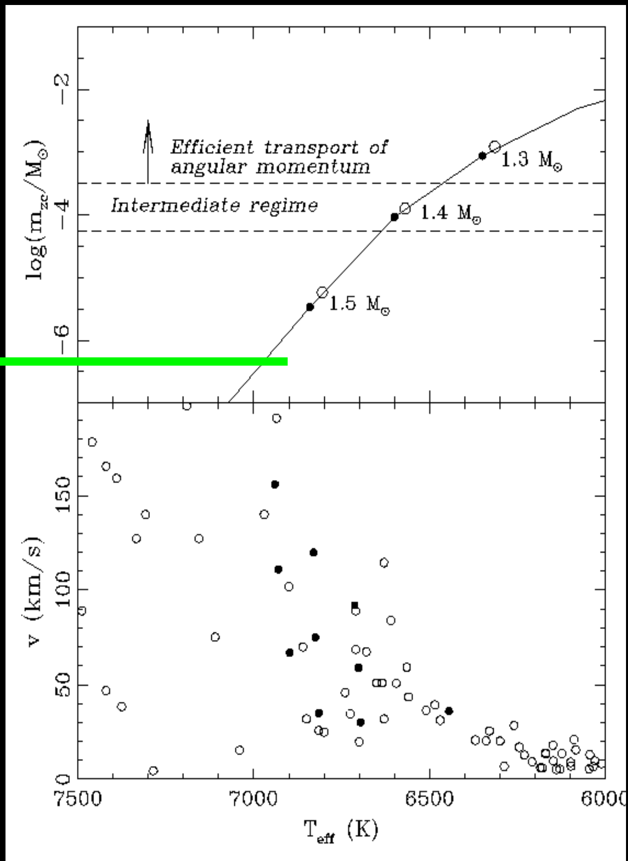

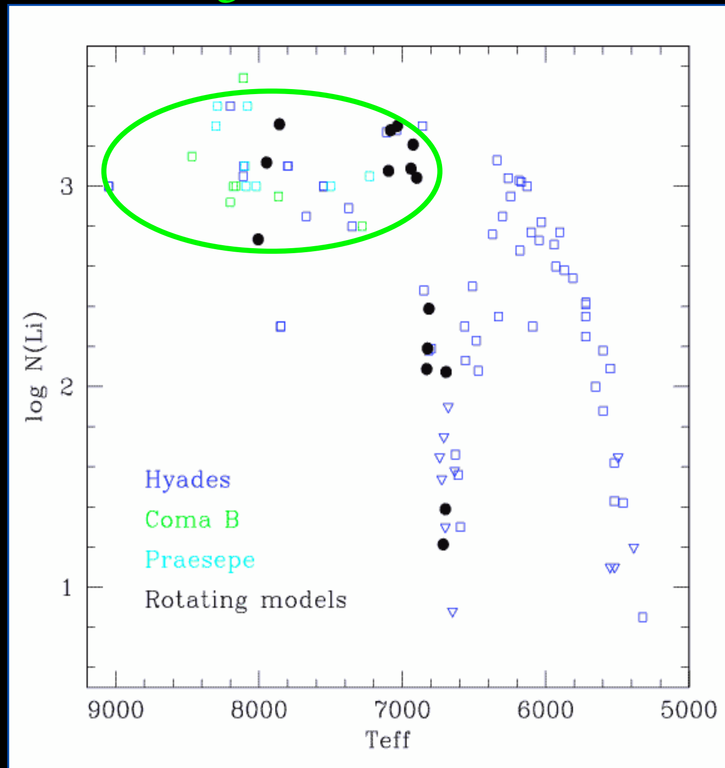

Talon & Charbonnel (98), Palacios et al. (03)

Rotation-induced mixing :
The hot side of the lithium dip

6600 K≤ Teff ≤ 6900 K : Deeper convective envelope
Weak magnetic torque slows down the outer layers

Angular momentum loss
drives circulation and depletes Li

Meridional circulation and shear increase
⇒ Larger destruction of Li

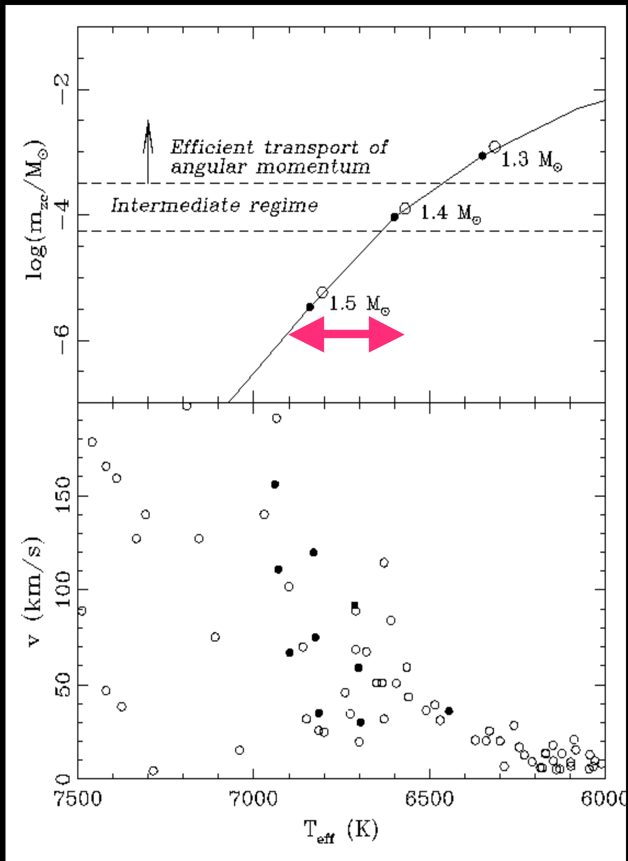

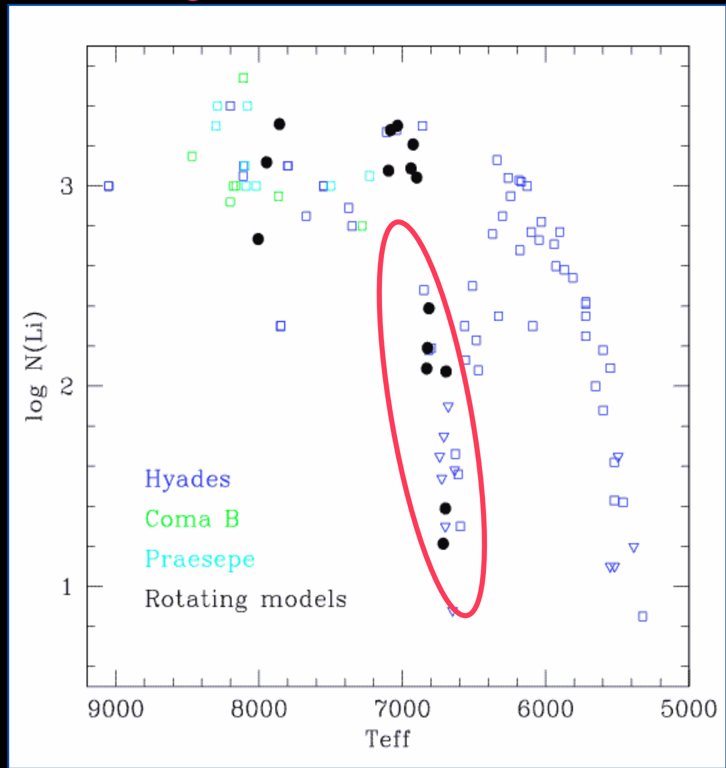

Talon & Charbonnel (98), Palacios et al. (03)

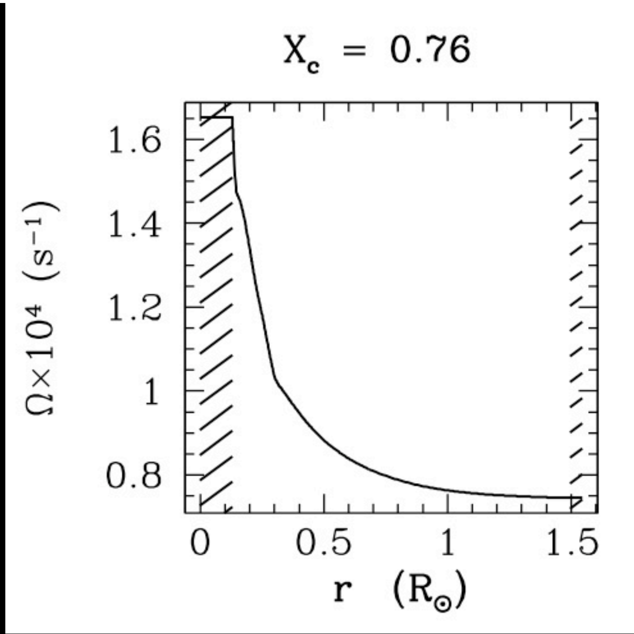

Angular velocity profile

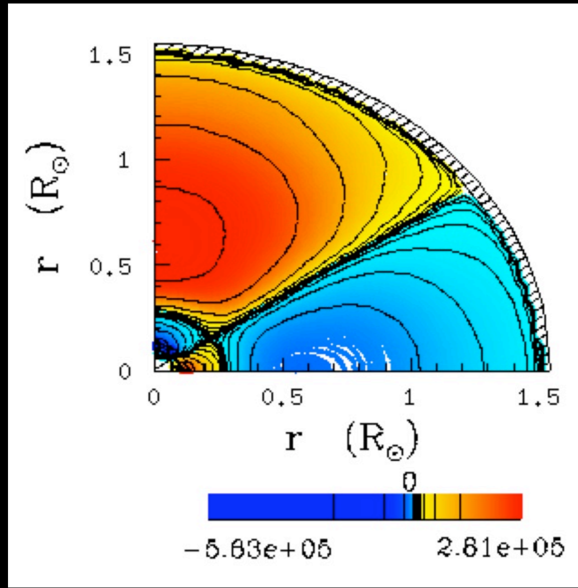

T-excesses

STAREVOL

Mathis et al. (06)

Decressin et al. (08)

$1.5 M_\odot$, $Z_\odot$

Vini=100 km s^{-1}

t (Hyades) :

Teff = 7020K

V = 80 km s^{-1}

Li = 2.9

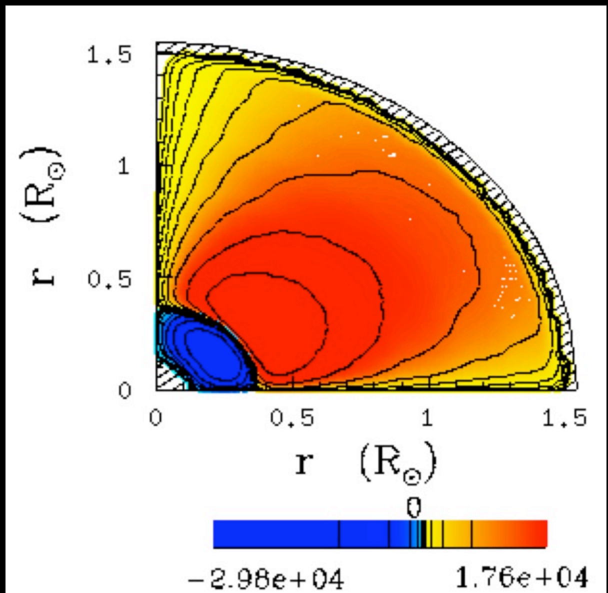

Meridional circulation currents

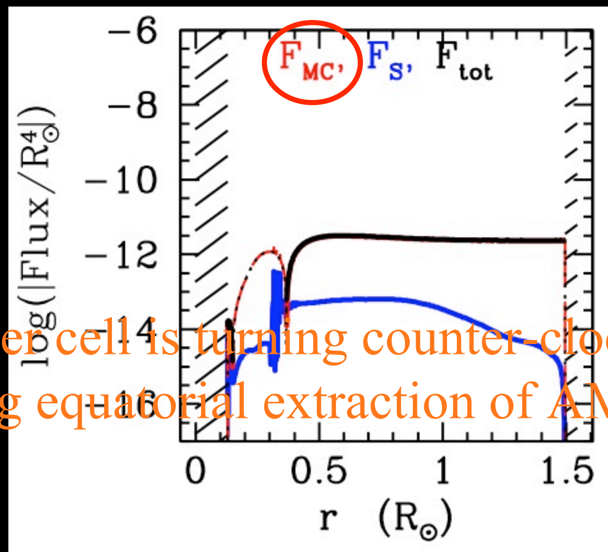

The outer cell is turning counter-clockwise
allowing equatorial extraction of AM by the wind

Flux of angular momentum

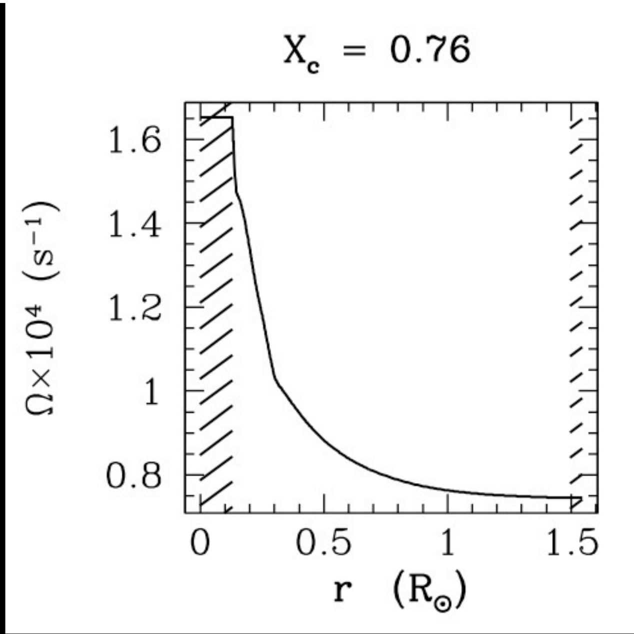

Angular velocity profile

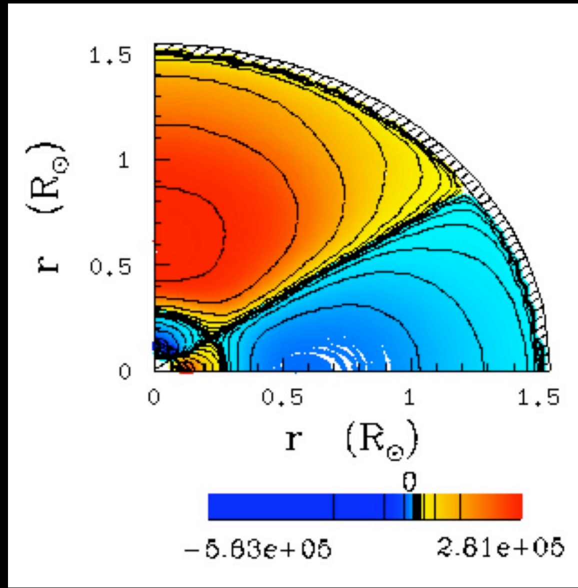

T-excesses

STAREVOL

Mathis et al. (06)

Decressin et al. (08)

$1.5 M_\odot$, $Z_\odot$

Vini=100 km s^{-1}

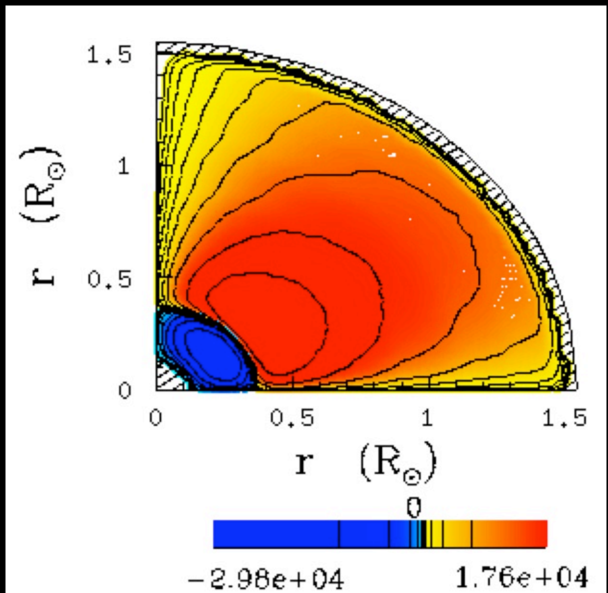

Meridional circulation currents

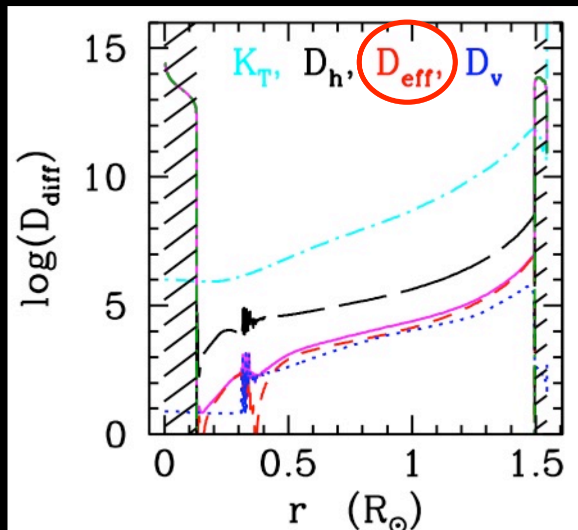

Transport of chemicals

Thermal diffusivity,
horizontal and
vertical
eddy-diffusivities,
effective (MC)
and total diffusivities

$D_h >> D_v$

Rotation-induced mixing :
The hot side of the lithium dip (MS)

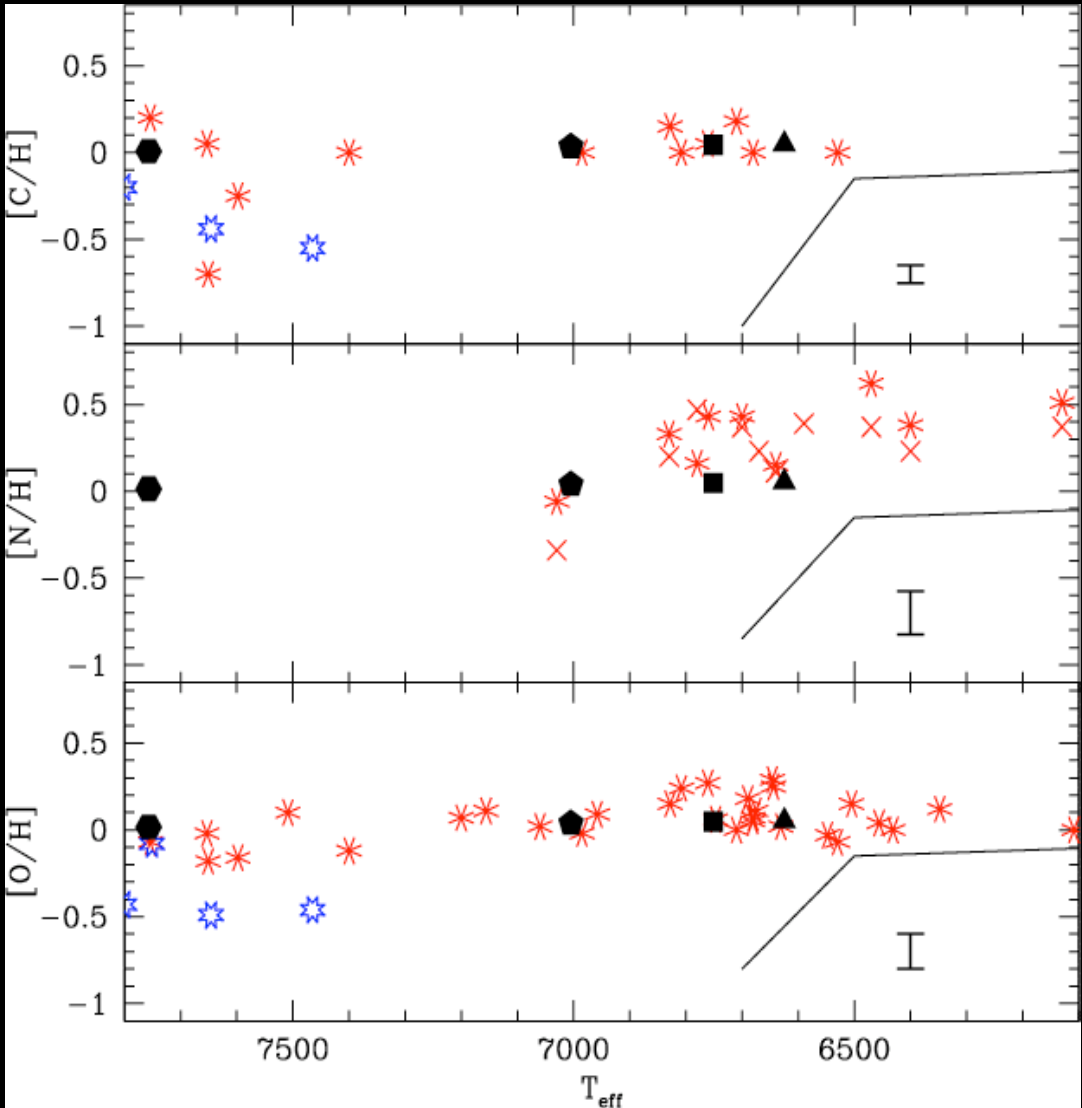

CNO at the age of the Hyades

Observations in the Hyades
Varenne & Monier (98)
Takeda et al. (98)

Solid lines : atomic diffusion alone
Turcotte et al. (98)

Rotating models : black points
Palacios et al. (03)

Palacios et al. (03)

Rotation-induced mixing :
The hot side of the lithium dip (MS)

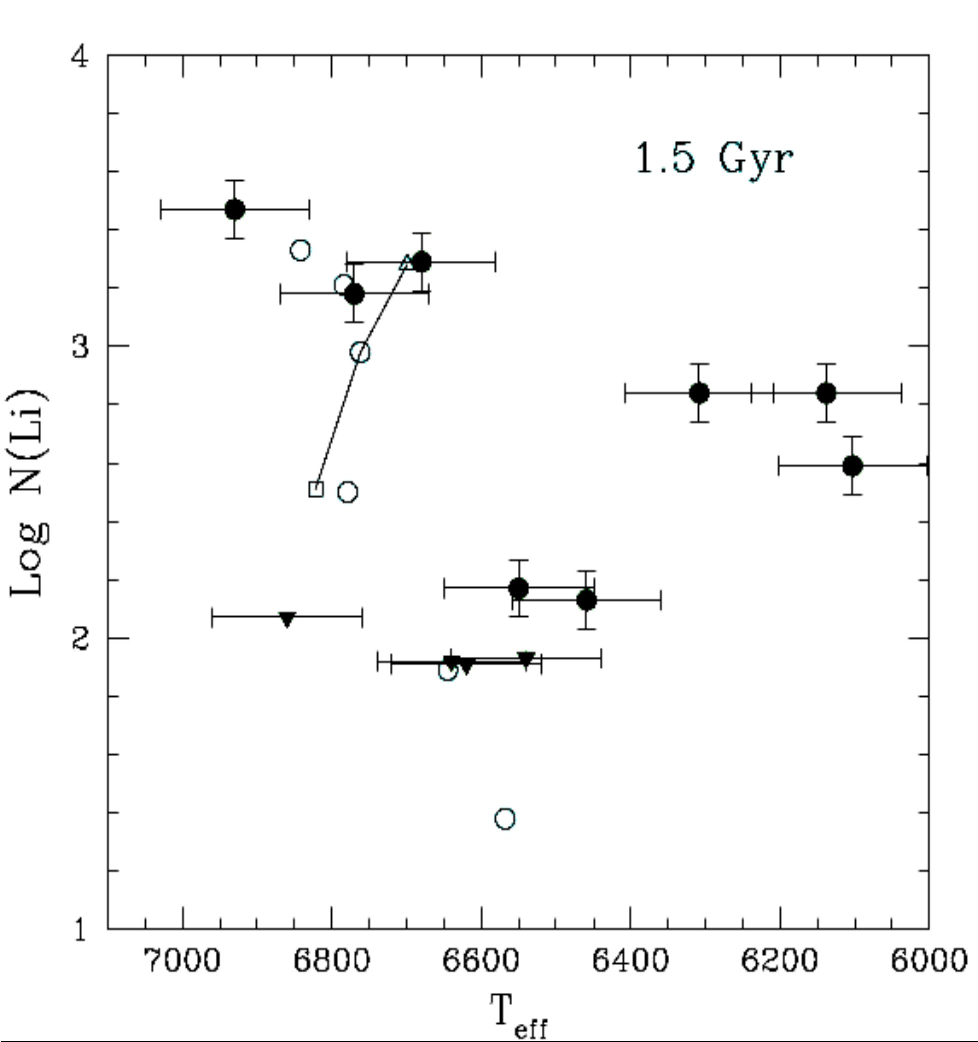

Li in IC 4651

Intermediate age, Mturnoff ~ 1.8$M_\odot$

Observations in IC 4651 : black points

Rotating models at 1.5 Gyr : open symbols
Vi = 110 km.sec^{-1}(+50 and 150 for the 1.5M_{sun})
(Charbonnel & Talon 99, Palacios et al. 03)

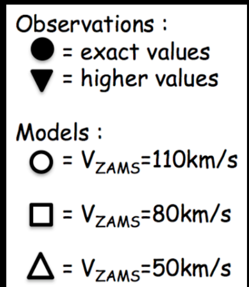

Pasquini, Randich, Zoccali, Hill, Charbonnel & Nordström (05)

Rotation-induced mixing : The hot side of the lithium dip (MS)

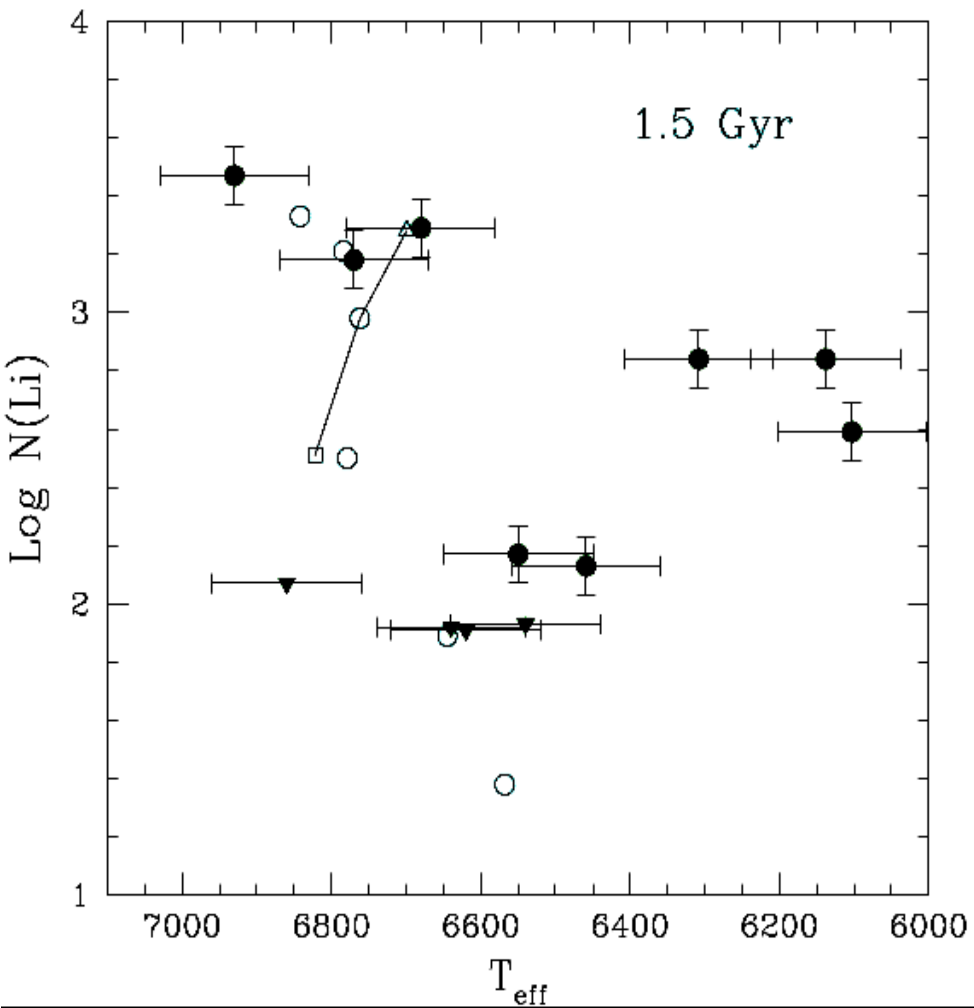

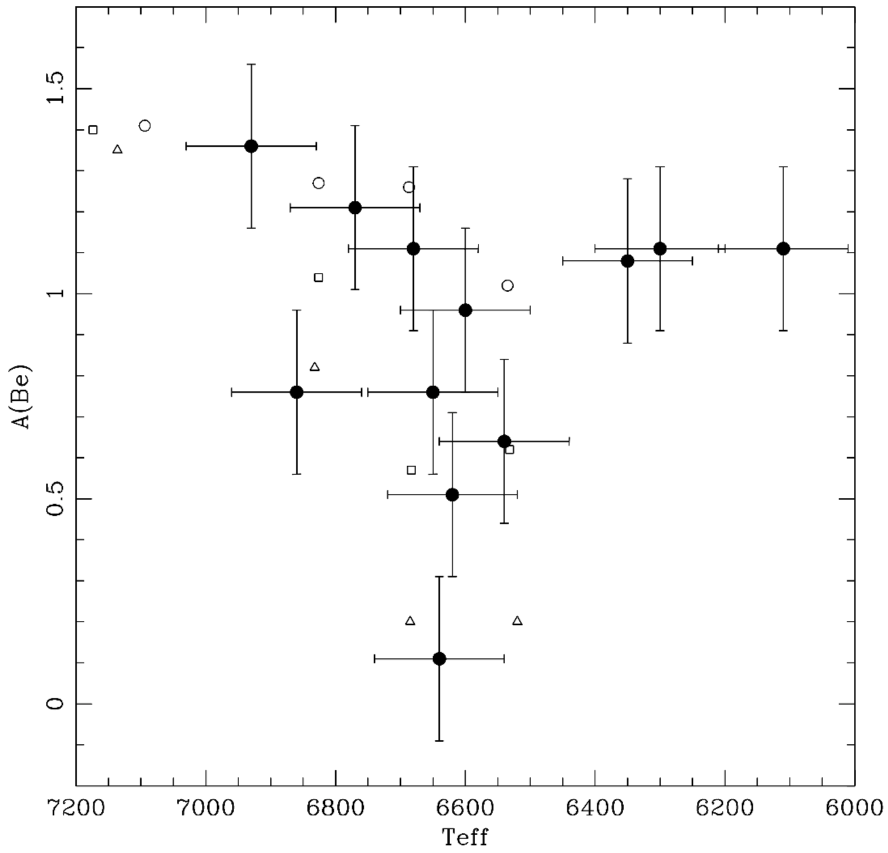

Smiljanic, Pasquini, Charbonnel, Lagarde (09)

Pasquini, Randich, Zoccali, Hill, Charbonnel & Nordström (05)

Rotation-induced mixing in low-mass main subgiant stars

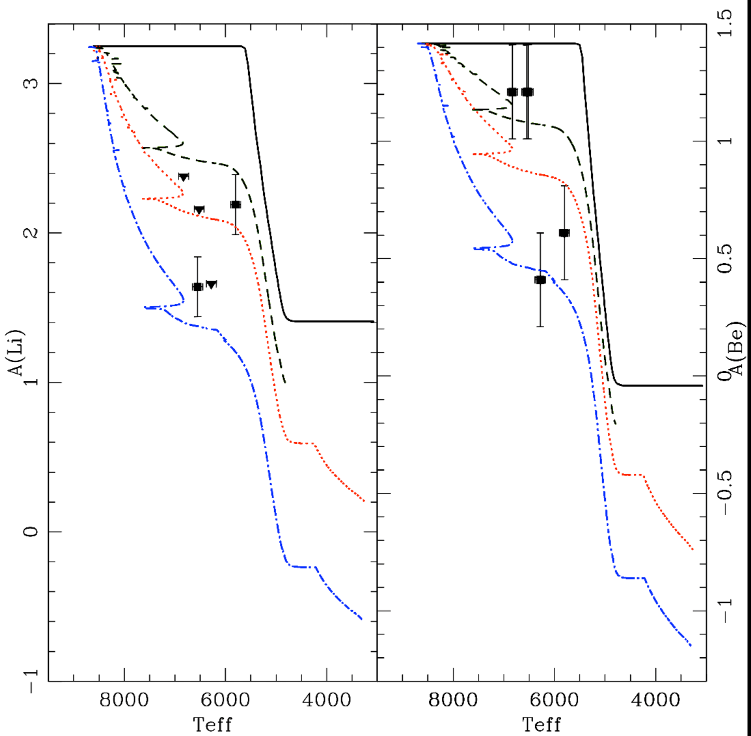

_____ Classical models

Models with thermohaline and rotation :

------ V_{ZAMS}=80 km/s

------ V_{ZAMS}=110km/s

------ V_{ZAMS}=180 km/s

Observations : IC 4651

Smiljanic, Pasquini, Charbonnel & Lagarde (09)

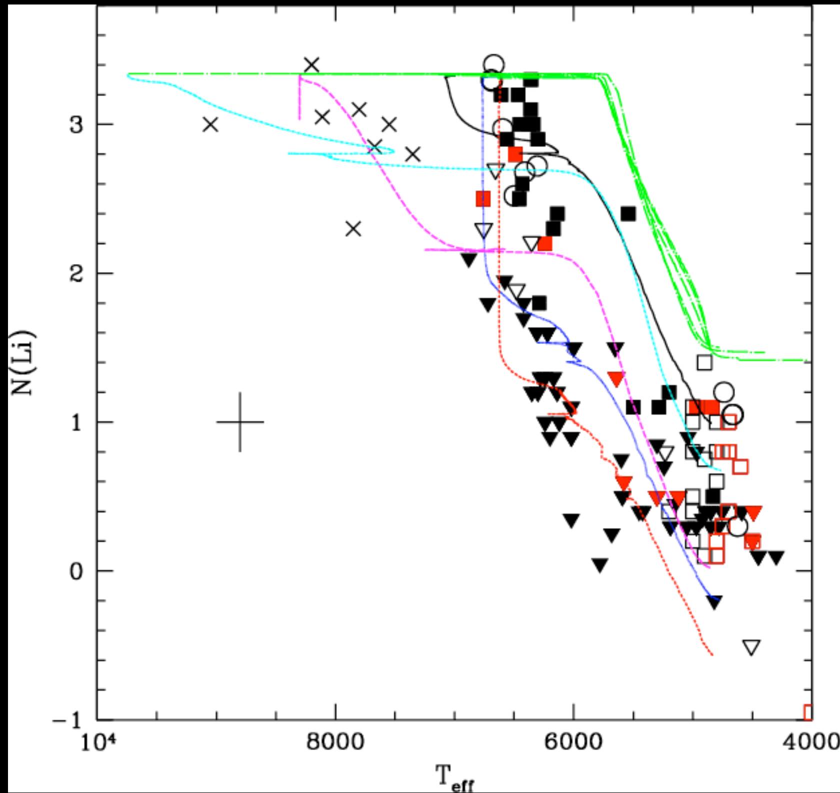

Standard models : green lines

Rotating models of various M_* : other colored lines

Observations : Field and
open cluster evolved stars

Lèbre et al. (99), Wallerstein et al. (94), Gilroy (89)
Pasquini et al. (01), Burkhart & Coupry (98, 00)

Palacios et al. (03), Pasquini et al. (04)

The rotating models
are successful
in explaining the data
for the stars lying on
or originating from
the hot side of the Li dip
(on a very large mass range!)

What about the less massive stars?

The cool side of the lithium dip

Teff ≤ 6600 K : Deep convective envelope sustaining strong dynamo
Strong magnetic torque
Very efficient magnetic braking of the outer layers

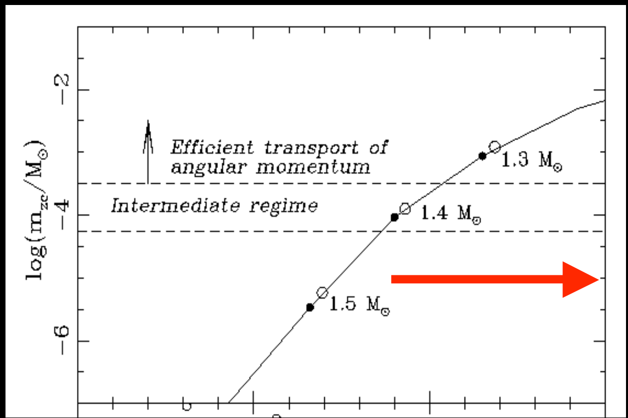

Meridional circulation and shear increase
⇒ Too much Li destruction

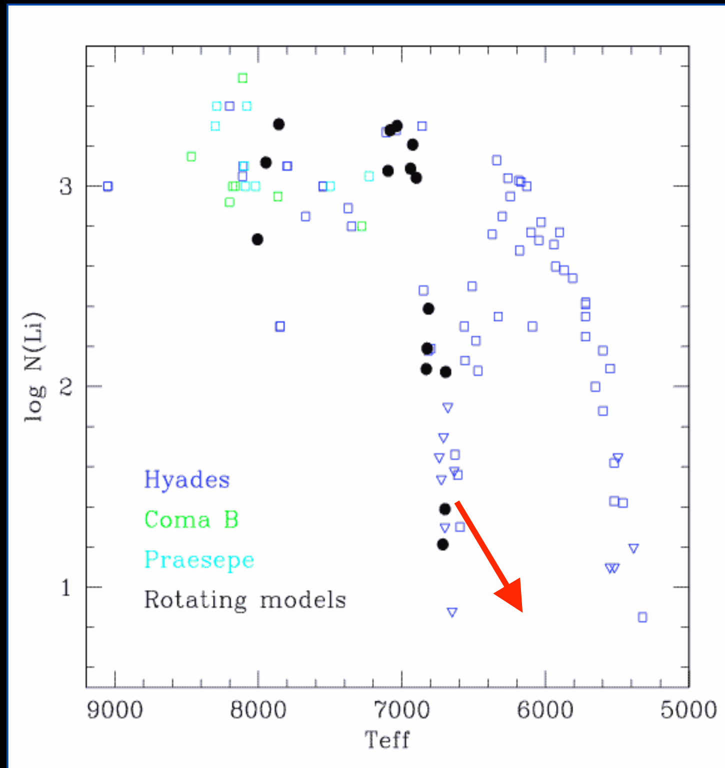

Another mechanism is very efficient in transporting angular momentum in cooler stars
(Talon & Charbonnel 98)

Clues from the solar case

Latitudinal differential rotation

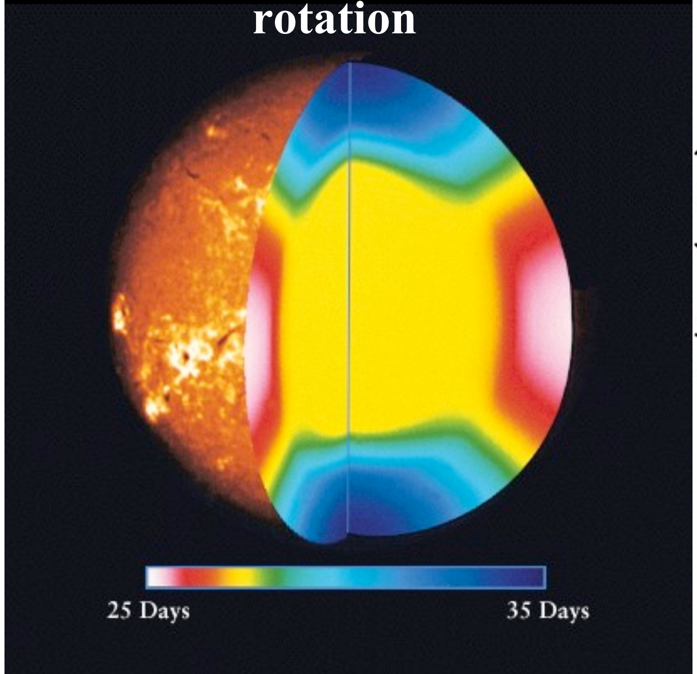

Brown et al. (89)
Kosovichev et al. (97)
Couvidat et al. (03)
…

Radial rotation profile

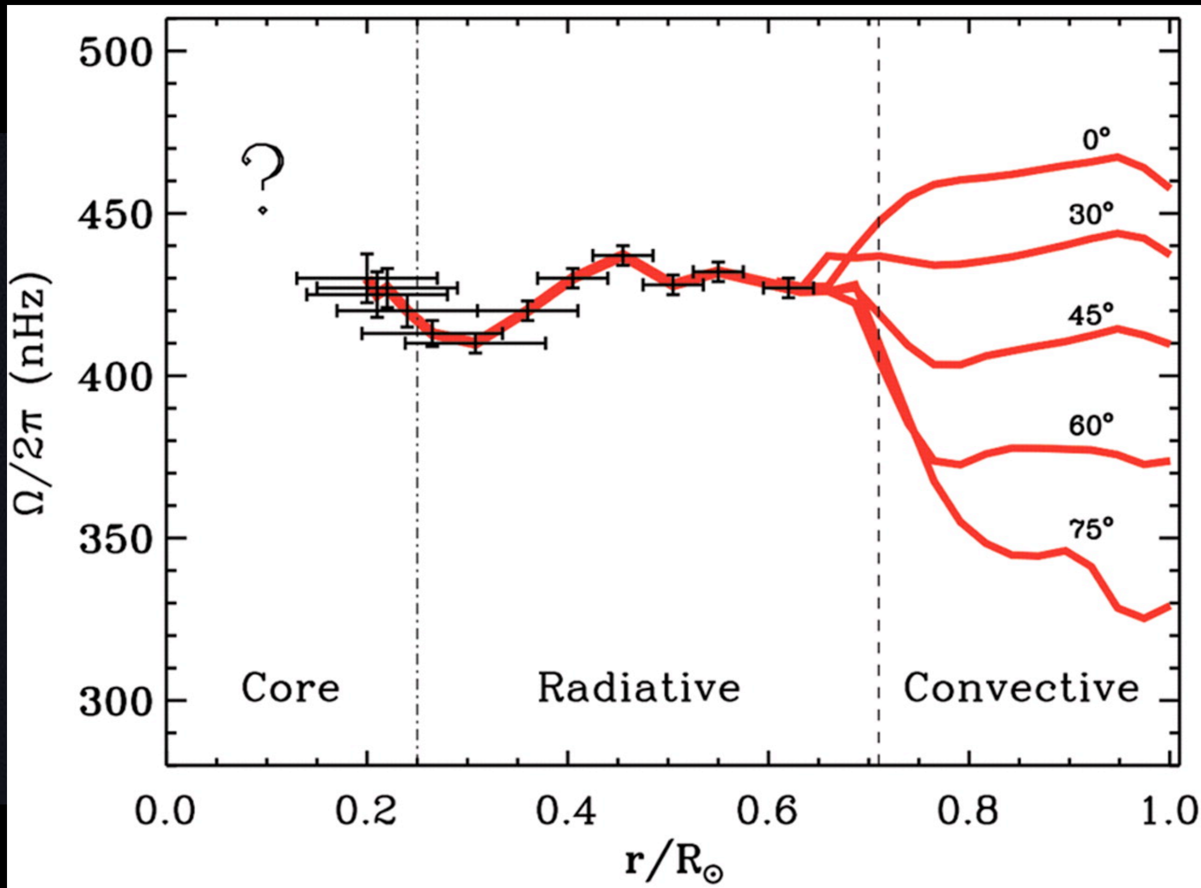

GOLF + MDI data

García et al. (07)

Clues from the solar case

Meridional circulation and shear turbulence
(Pinsonneault et al. 89, Chaboyer et al. 95, Zahn et al. 97)
fail to extract sufficient angular momentum from the radiative interior to explain the ~ flat rotation profile in the Sun **(Brown et al. 1989)**

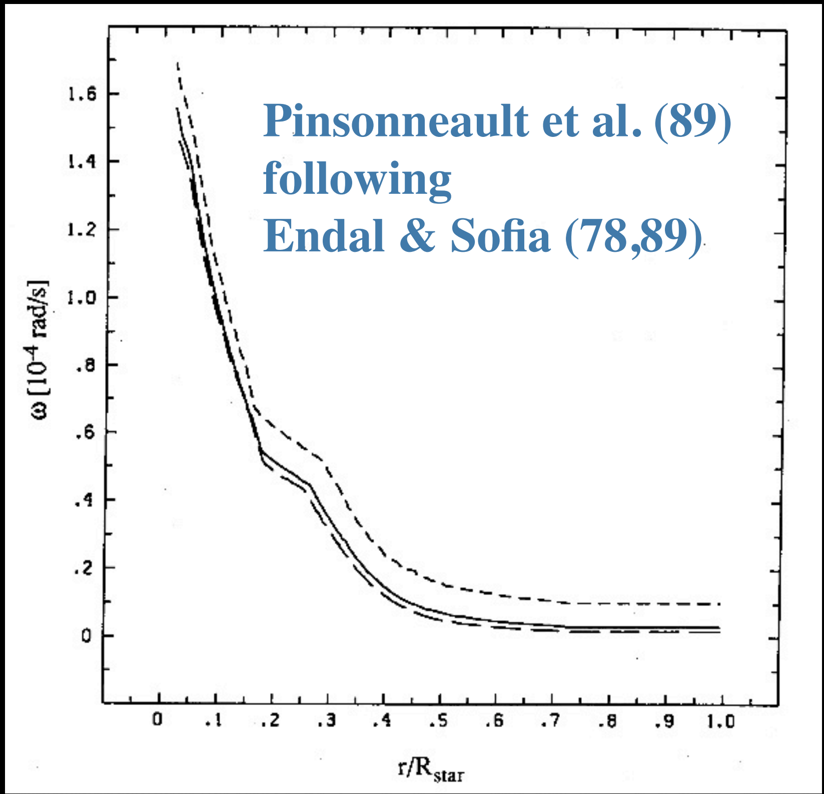

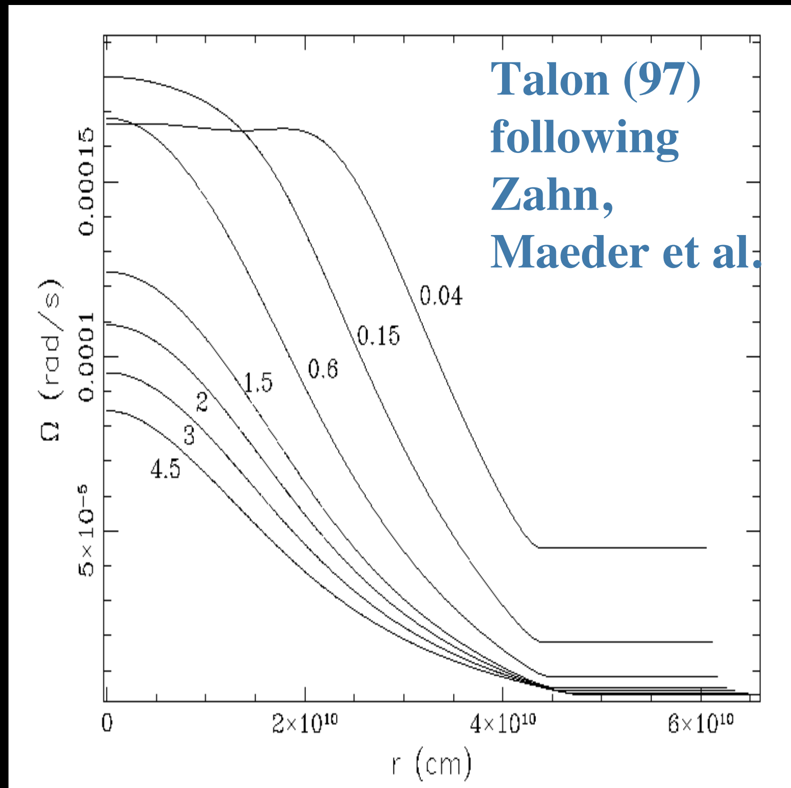

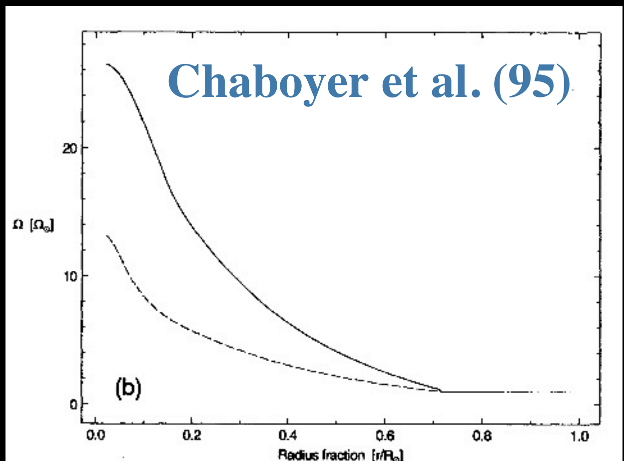

Clues from the solar case

Meridional circulation and shear turbulence
(Pinsonneault et al. 89, Chaboyer et al. 95, Zahn et al. 97)
fail to extract sufficient angular momentum from the radiative interior to explain the ~ flat rotation profile in the Sun (Brown et al. 1989)

Sun and cool side of the Li dip → Angular momentum transported by

Magnetic fields ?
Charbonneau & Mc Gregor 93, Barnes et al. 97, Eggenberger et al. 05

→No correlation is expected with Teff

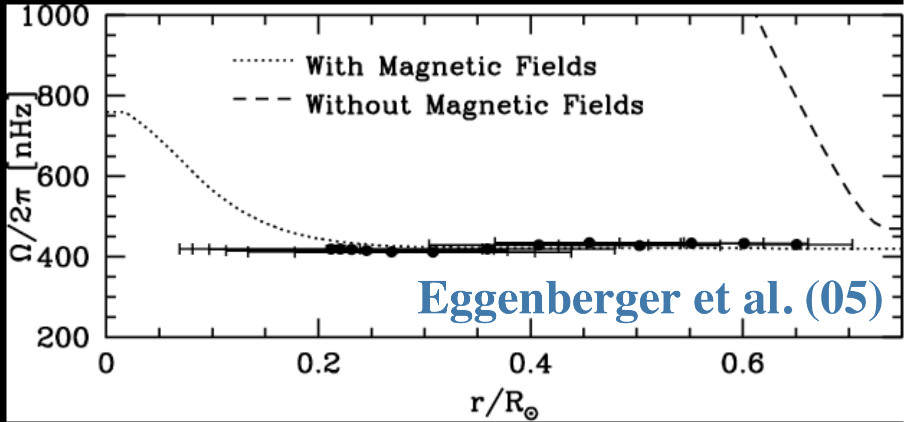

Internal gravity waves ?
Schatzman 1993, Zahn et al. 97, Kumar & Quataert 97, Kumar et al. 99, Talon et al. 02, Talon & Charbonnel 03,04

→ Efficiency dependent on the convection envelope characteristics, as required by the Li data

Internal Gravity Waves

Earth's atmosphere
Wind compression by topography
→ Cloud patterns formed in the regions of low-P of a topography wave

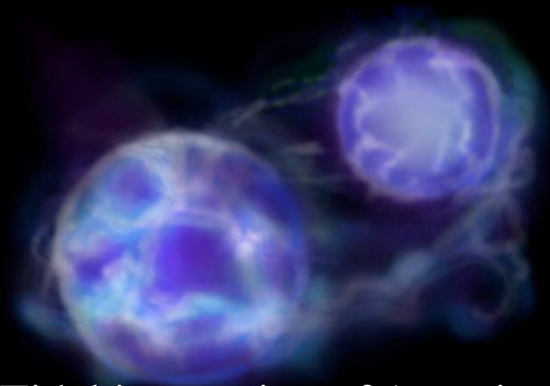

Tidal interaction of (massive) **binary systems**
Zahn (70, 75, 76), Goldreich & Nicholson (89)

Excitation of internal Gravity Waves

- In single stars, IGWs are produced by the injection of kinetic energy from a turbulent (convection) region to a stable adjacent region. Two sources of excitation:

  - **Convective overshooting in the adjacent radiative zone**

    García-López & Spruit 91; Frits et al. 98; Kiraga et al. 03; Rogers & Glatzmaier 05

  - **Reynolds stresses in the convection zone itself**

    Goldreich & Keeley 77; Goldreich & Kumar 90; Goldreich et al. 94 (GMK)

  → First applied to solar p-modes; reproduces the solar spectral energy input rate distribution; driving is dominated by entropy fluctuations

  Balmforth 92

Looking for realistic wave fluxes from numerical simulations !

Wave Excitation in 2-3D numerical simulations of penetrative convection

See also
Hurlburt et al. (86, 94)
Andersen (94)
Nordlund et al. (96)
Kiraga et al. (00, 03)
Dintrans et al. (05)
Rogers & Glatzmaier (05)

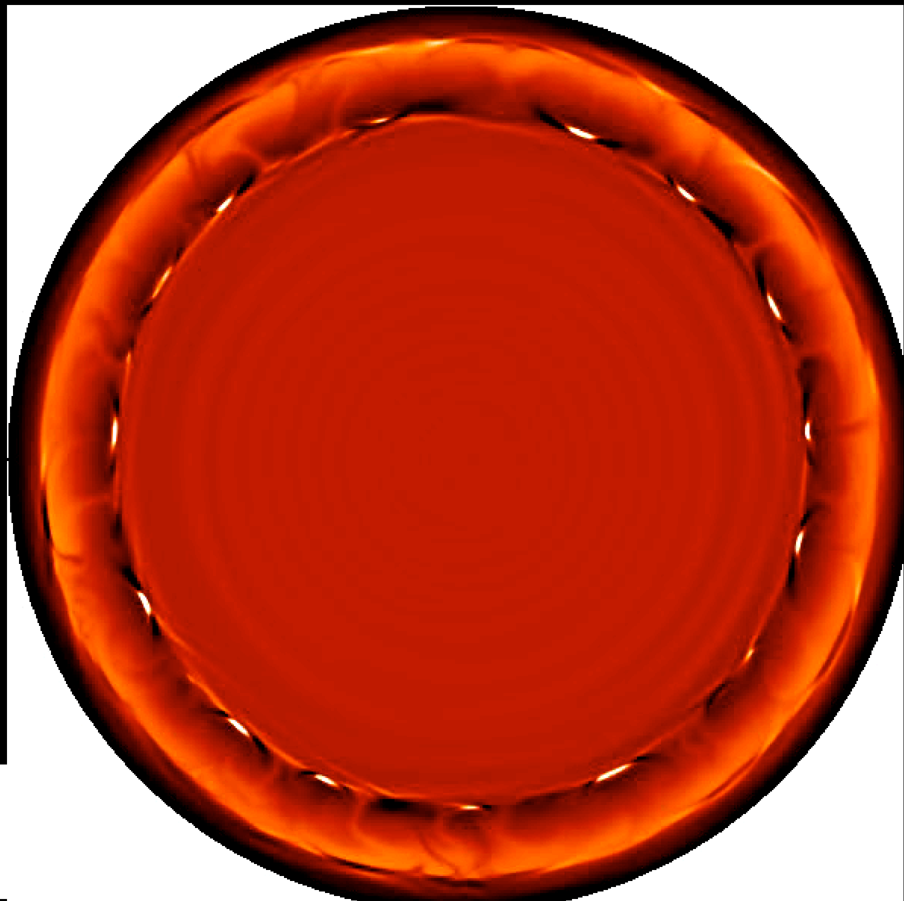

Temperature fluctuation

Rogers & Glatzmaier (06)
Wave Excitation in a cylindrical (2D) model with stratification similar to that of the Sun

? Is the level of turbulence reached in the simulation realistic ?

? Analysis of the wave spectrum as a function of convective properties (i.e., vs Teff) ?

For the moment, we still have to rely on theoretical estimates for wave generation

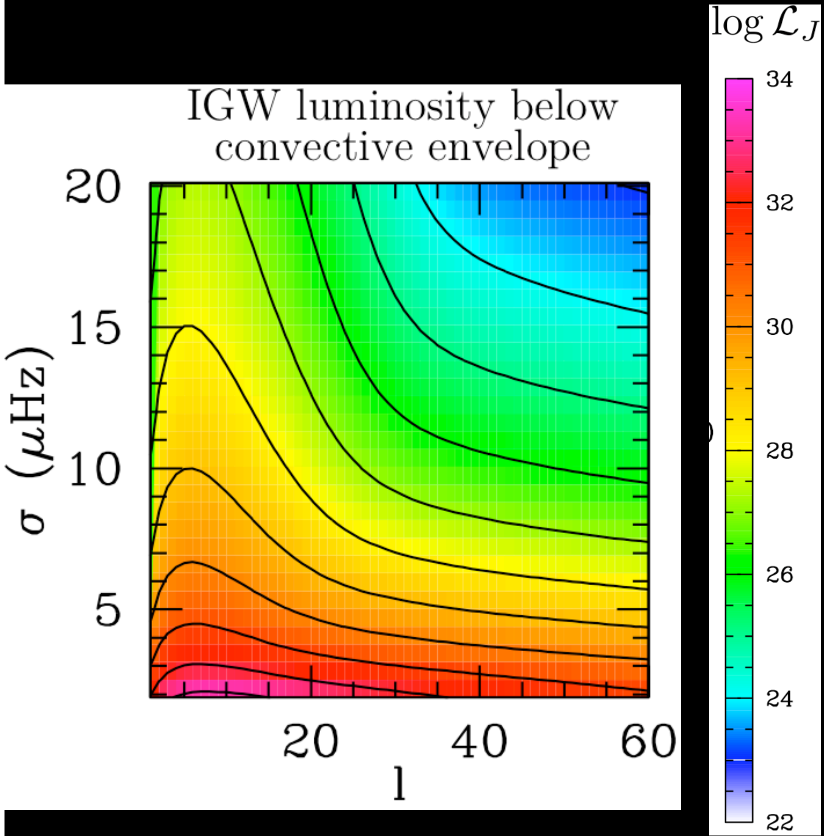

Spectrum of IGW luminosity
below the CE
generated by Reynolds stresses
$1.1M_\odot$, $Z_\odot$ at 180 Myrs

Volume excitation model of Goldreich et al. (94) is used for the kinetic energy flux $\mathscr{F}_J$ (driving is dominated by entropy fluctuations)

↓

Wave spectrum of angular momentum luminosity ($4\pi r^2 \mathscr{F}_J$) just below the convective envelope

Frequency σ ≤ Brunt-Vaïsälä frequency
(natural oscillation frequency of a displaced element in a stratified region)
Order l ≤ lc, spherical order characterizing convection
(corresponds to the pressure scale-height)

Mathis, Decressin, Eggenberger & Charbonnel (in prep.)
following Talon, Kumar & Zahn (02), Kumar & Quataert (97), Talon & Charbonnel (03, 04, 05)

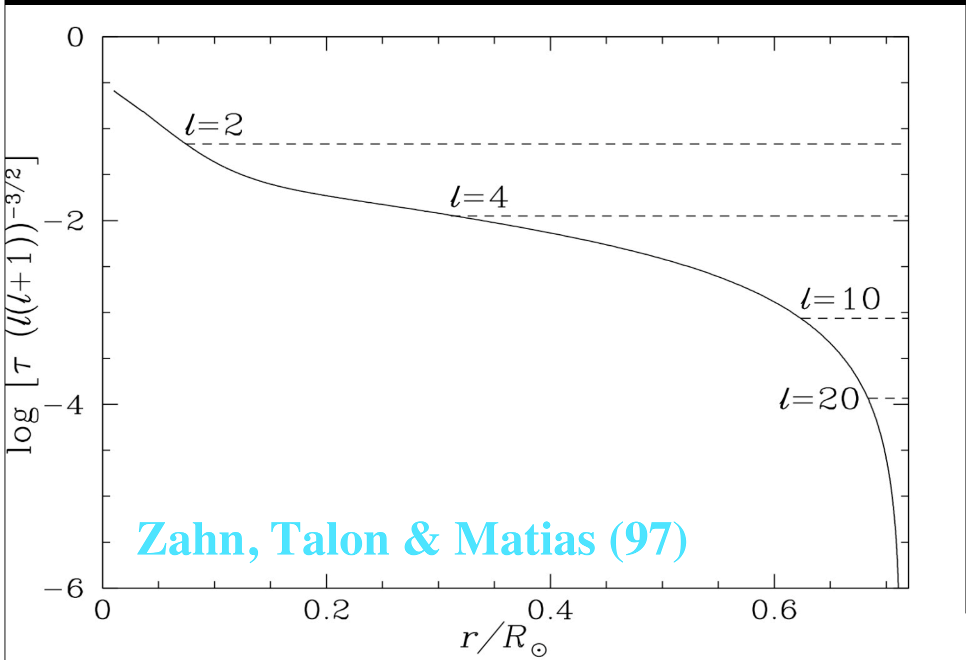

Evaluation of the **damping factor τ** for a frequency of 1μHz in a solar model.

The depth corresponding to an attenuation by a factor 1/e is shown for various degrees ℓ

Local momentum luminosity integrated over the whole spectrum :

$$\mathcal{L}_J(r) = \sum_{\sigma,\ell,m} \underbrace{\mathcal{L}_{J\ell,m}(r_{cz})}_{\alpha F_{conv}} \exp\left[-\tau(r,\sigma,\ell)\right]$$

$$\tau(r,\sigma,\ell) = [\ell(\ell+1)]^{\frac{3}{2}} \int_r^{r_c} \underbrace{(K_T+\nu_v)}\ \frac{N N_T{}^2}{\sigma^4} \left(\frac{N^2}{N^2-\sigma^2}\right)^{\frac{1}{2}} \frac{dr}{r^3}$$

Integrated damping due to thermal diffusion K_T and turbulent viscosity ν_t

σ : local frequency

$N^2 = N^2_T + N^2$: Brunt-Väisälä frequency

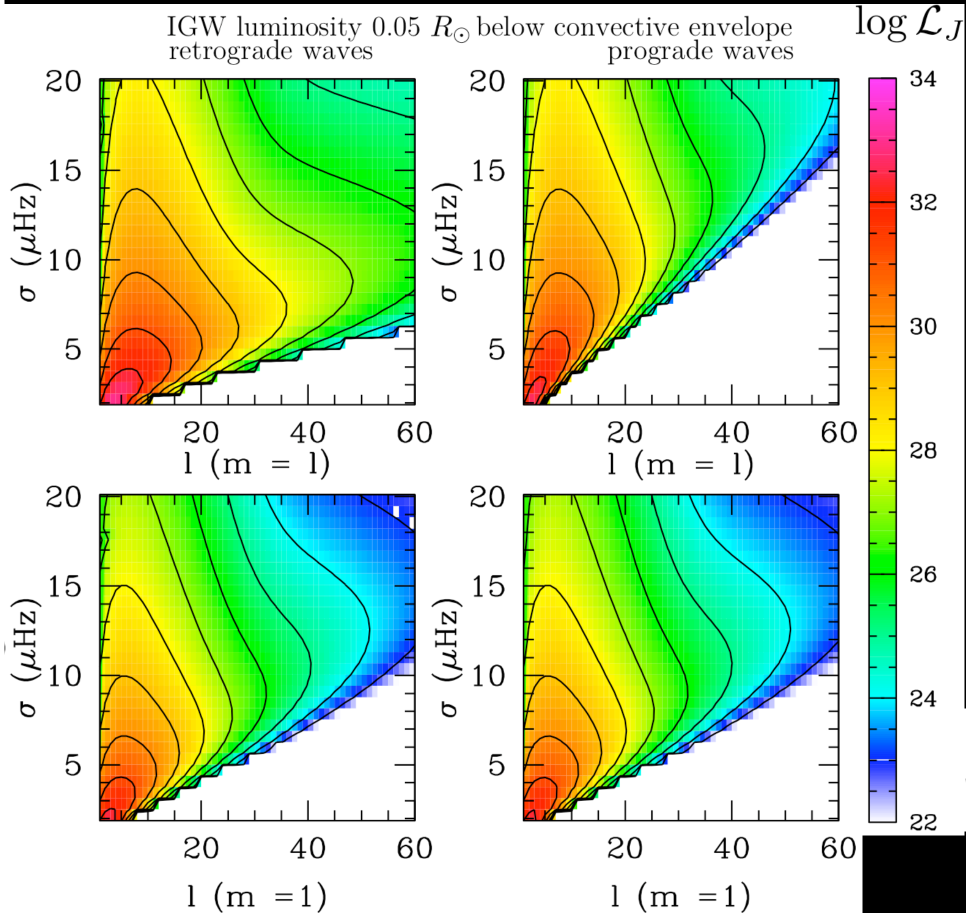

Wave spectrum of angular momentum luminosity at 0.05 R below the convective envelope - 1.1M$_\odot$, Z$_\odot$ at 180 Myrs

Local momentum luminosity integrated over the whole spectrum :

$$\mathcal{L}_J(r) = \sum_{\sigma,\ell,m} \underbrace{\mathcal{L}_{J\ell,m}(r_{cz})}_{\alpha F_{conv}} \exp\left[-\tau(r,\sigma,\ell)\right]$$

$$\tau(r,\sigma,\ell) = \left[\ell(\ell+1)\right]^{\frac{3}{2}} \int_r^{r_c} \underbrace{(K_T + \nu_v)} \frac{N N_T{}^2}{\sigma^4} \left(\frac{N^2}{N^2-\sigma^2}\right)^{\frac{1}{2}} \frac{dr}{r^3}$$

Integrated damping due to thermal diffusion K_T and turbulent viscosity ν_t

σ : local frequency

$N^2 = N^2_T + N^2$: Brunt-Väisälä frequency

Mathis, Decressin, Eggenberger & Charbonnel (in prep.)
following Talon, Kumar & Zahn (02), Kumar & Quataert (97), Talon & Charbonnel (03, 04, 05)

Spectrum of IGW luminosity generated by Reynold stress - 1.1$M_\odot$ at 180 Myrs

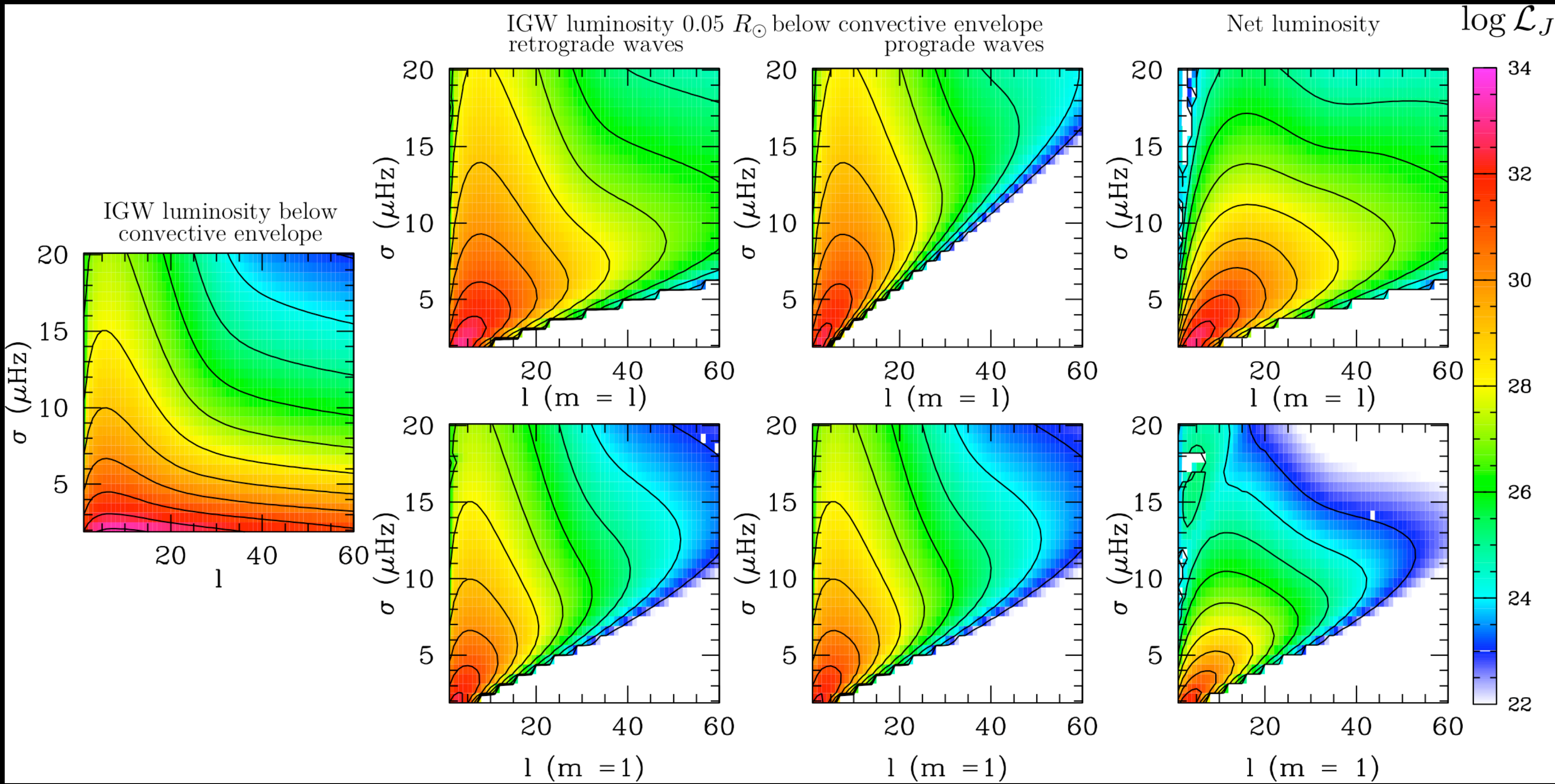

✓ Most of the momentum is carried by low-frequency waves

✓ Significant momentum luminosity in low-order waves that penetrate deep into the interior

Mathis, Decressin, Eggenberger & Charbonnel (in prep.)
following Talon, Kumar & Zahn (02), Kumar & Quataert (97), Talon & Charbonnel (03, 04, 05)

$\mathbf{L_J}$: Net momentum luminosity
at $0.03R_*$ below the surface convection zone
as a function ot Teff (zams) for Pop I stars
⇔Momentum extraction in the stellar interior

Local momentum luminosity integrated over the whole spectrum :

$$\mathcal{L}_J(r) = \sum_{\sigma,\ell,m} \underbrace{\mathcal{L}_{J\ell,m}(r_{cz})}_{\alpha\, F_{conv}} \exp\left[-\tau(r,\sigma,\ell)\right]$$

Momentum transport by IGW
has the proper mass dependence
to be the required process

Local amplitude :

$$\tau(r,\sigma,\ell) = [\ell(\ell+1)]^{\frac{3}{2}} \int_r^{r_c} \underbrace{(K_T + \nu_v)}\, \frac{N N_T{}^2}{\sigma^4} \left(\frac{N^2}{N^2-\sigma^2}\right)^{\frac{1}{2}} \frac{dr}{r^3}$$

Integrated damping due to thermal diffusion K_T and turbulent viscosity ν_t
σ : local frequency
$N^2 = N^2_T + N^2$: Brunt-Väisälä frequency

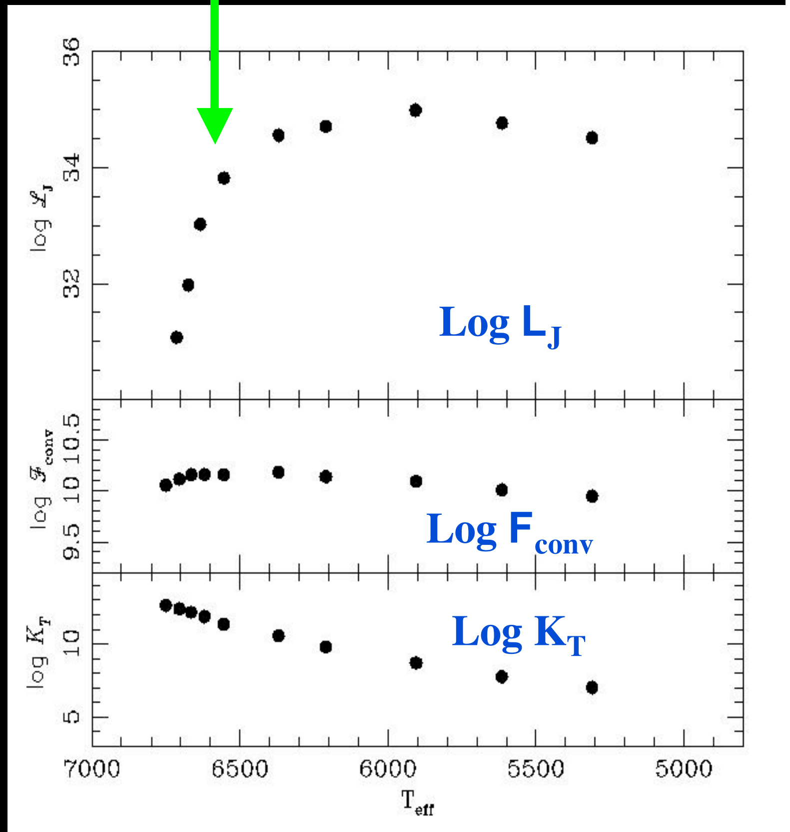

Talon & Charbonnel (03, 04)

Complete evolution models including rotation, gravity waves and atomic diffusion

Transport of angular momentum :

$$\frac{\mathrm{d}}{\mathrm{d}t}\left[r^2\Omega\right] = \frac{1}{5r^2}\frac{\partial}{\partial r}\left[\, r^4\Omega U_2\right] + \frac{1}{r^2}\frac{\partial}{\partial r}\,\nu r^4\frac{\partial\Omega}{\partial r} - \frac{3}{8\pi}\frac{1}{r^2}\frac{\partial\mathcal{L}_J(r)}{\partial r}$$

Contraction or expansion — Advection (MC) — Diffusion (shear) — IGW

Local momentum luminosity
is obtained by calculating the damping integral for each individual waves
and then summing over all waves

Rotation profile inside a 1.0 $M_\odot$, Z=0.02 star

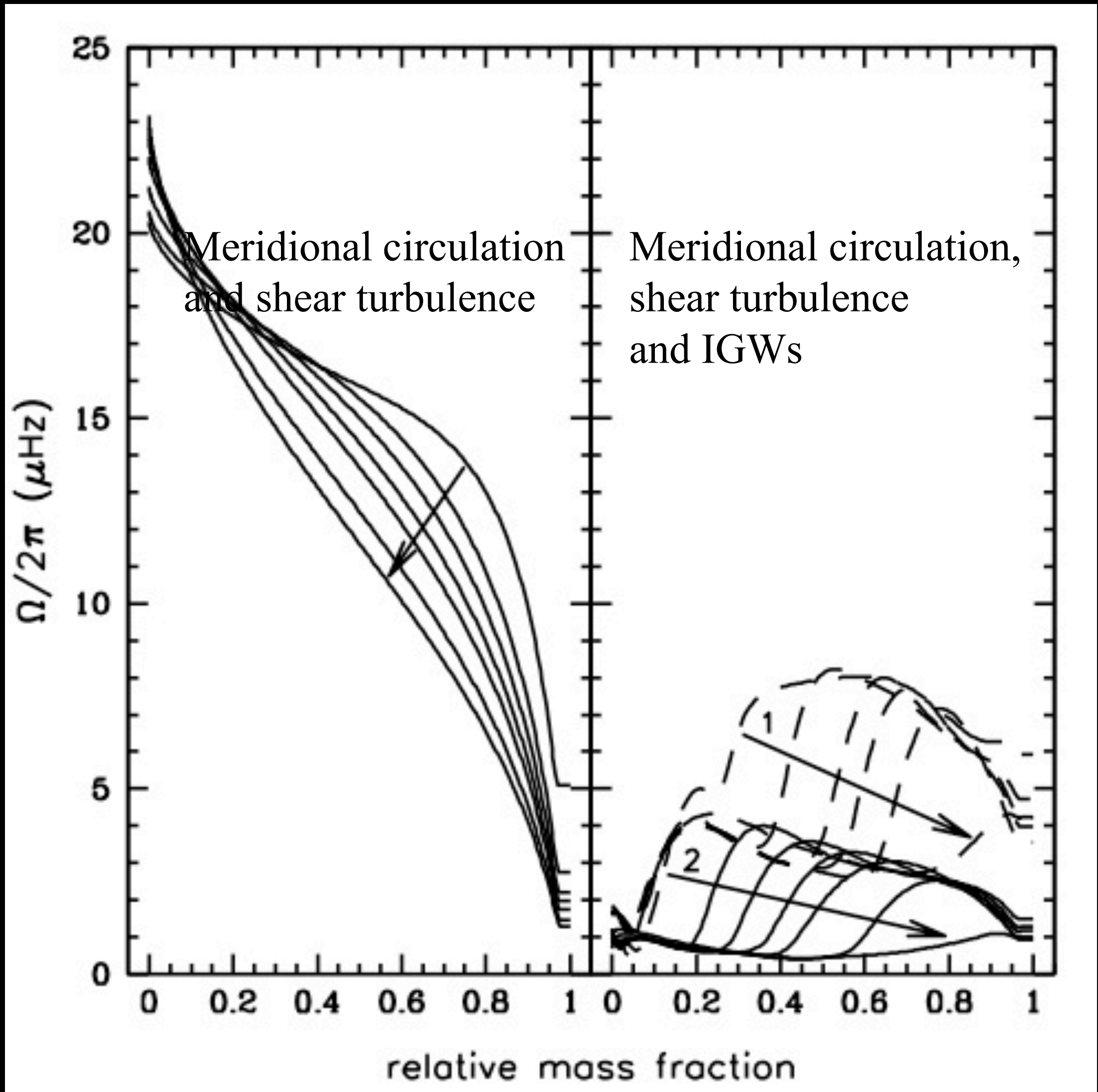

Identical magnetic braking applied
Vi = 50 km s^{-1}

Charbonnel & Talon (05)

1M$_\odot$, Z=0.02

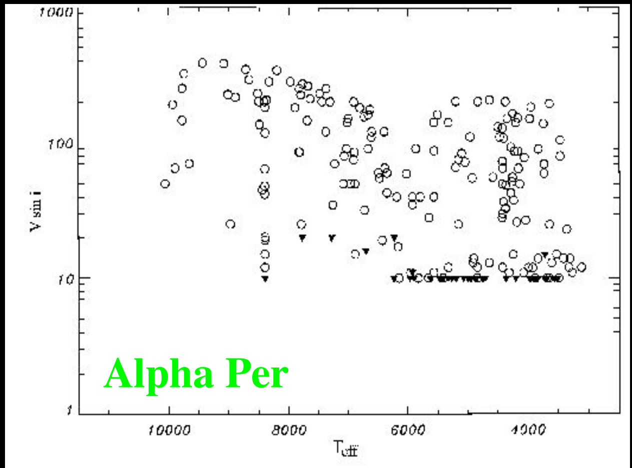

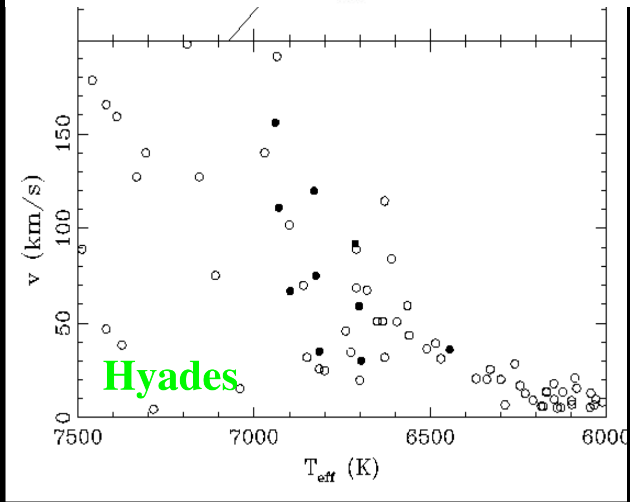

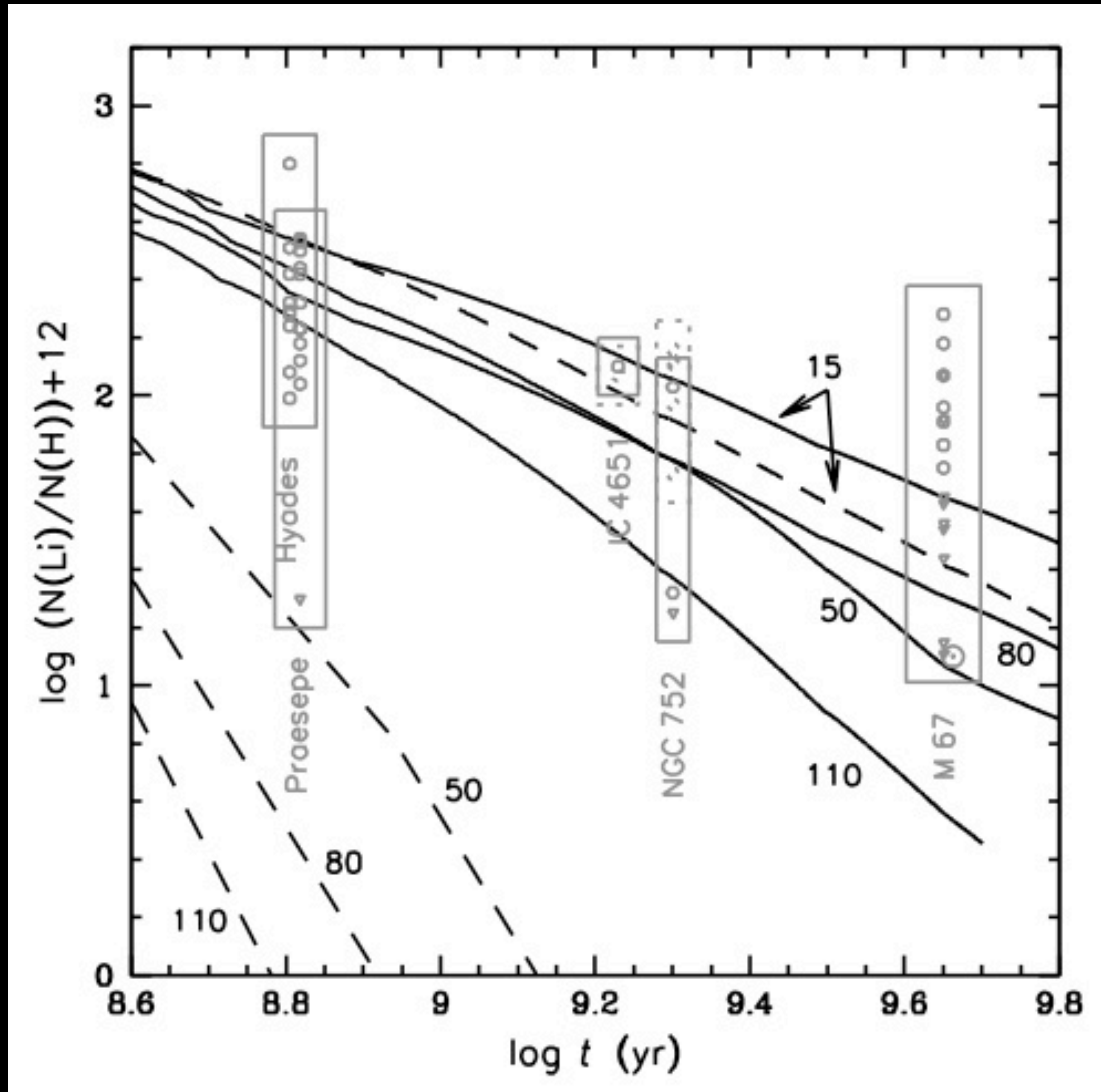

Magnetic braking applied
with Kawaler (1988) formulation

MC and shear turbulence
MC, shear and IGWs

Charbonnel & Talon (05)

$1M_{\odot}$, Z=0.02

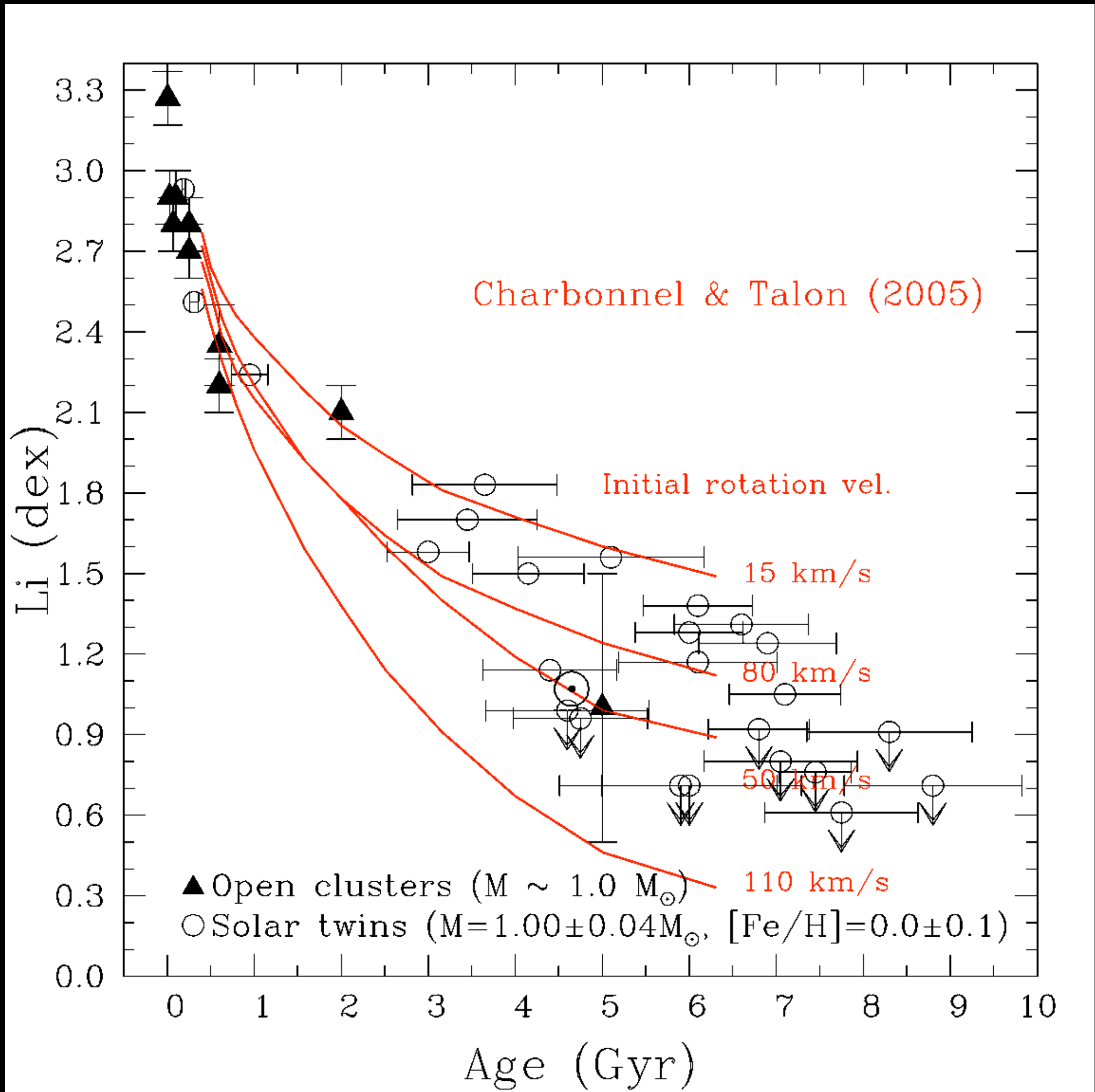

Melendez et al. (09)

Pre-main sequence

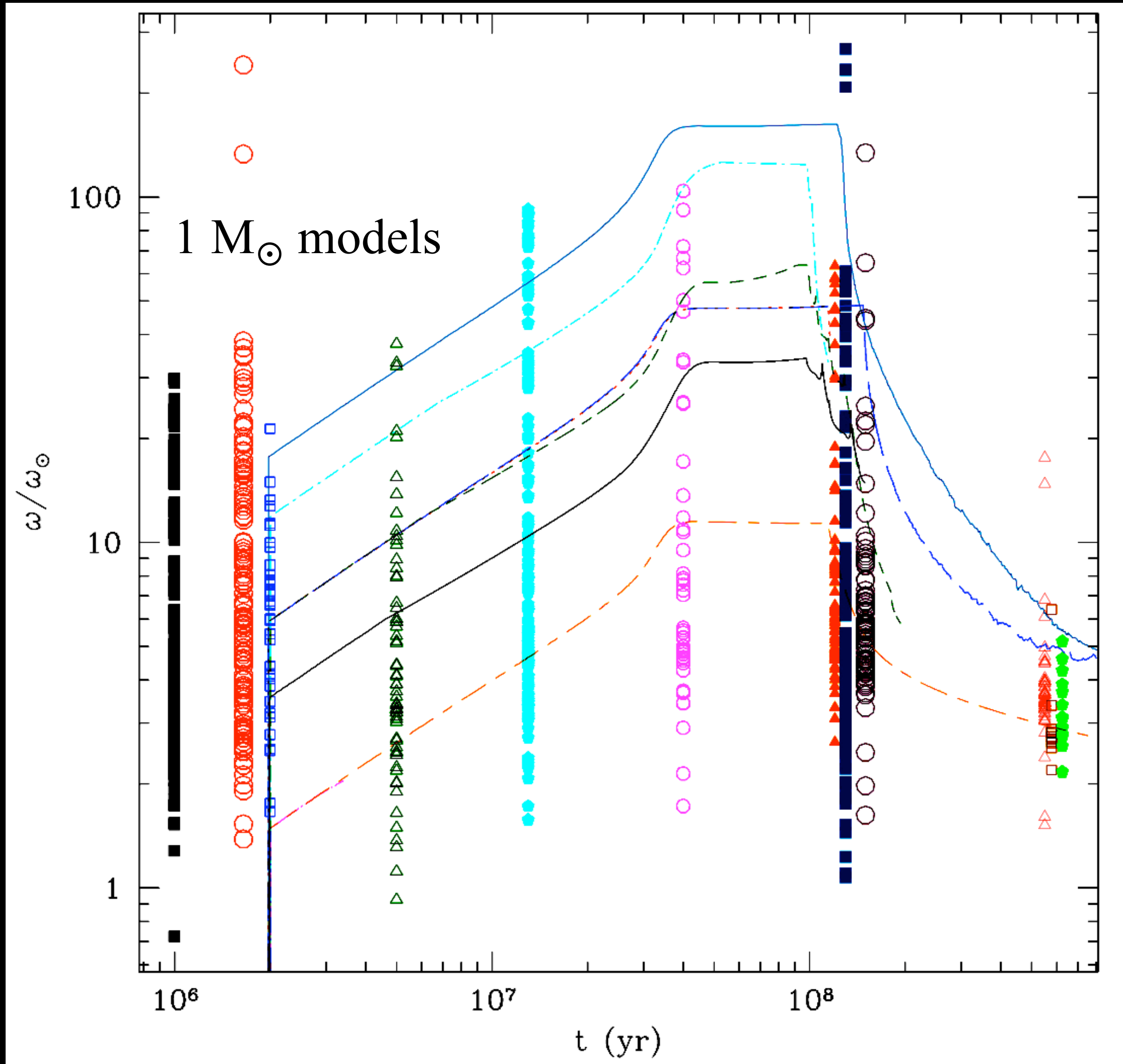

Data: Rotational periods in young open clusters (0.9 - 1.1$M_\odot$)
Gallet & Bouvier (in prep)

Charbonnel, Decressin & Talon (in prep.)

Pre-main sequence

$1M_\odot$
V_i = 20 km/sec
$Prot_i$ = 5 d
Vzams = 102 km/sec

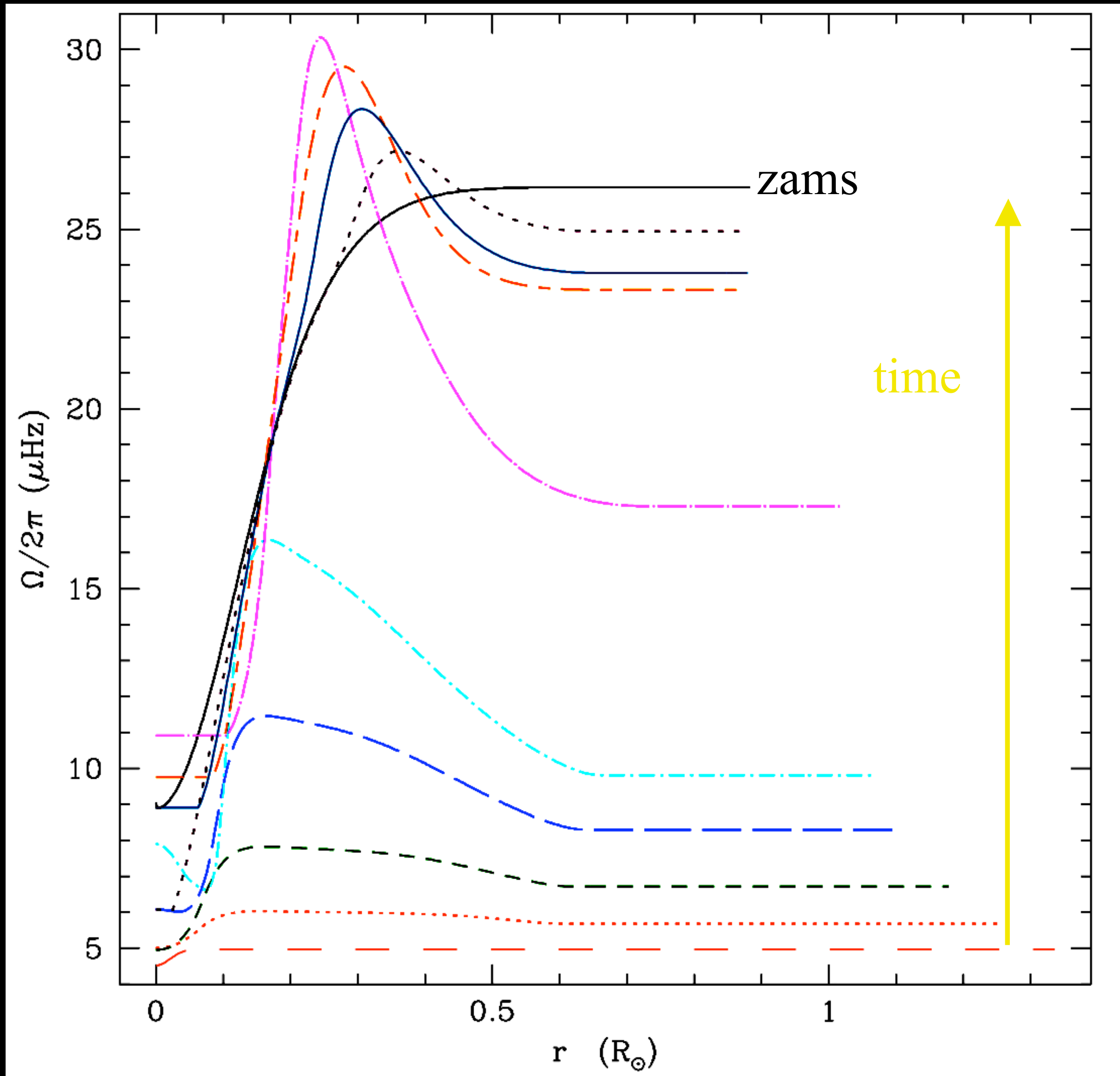

6.2, 8, 11, 16, 22, 36, 51, 65, 80, 98 Myr

Charbonnel, Decressin & Talon (in prep.)

Main sequence

$1M_\odot$
V_i = 20 km/sec
$Prot_i$ = 5 d
Vzams = 102 km/sec

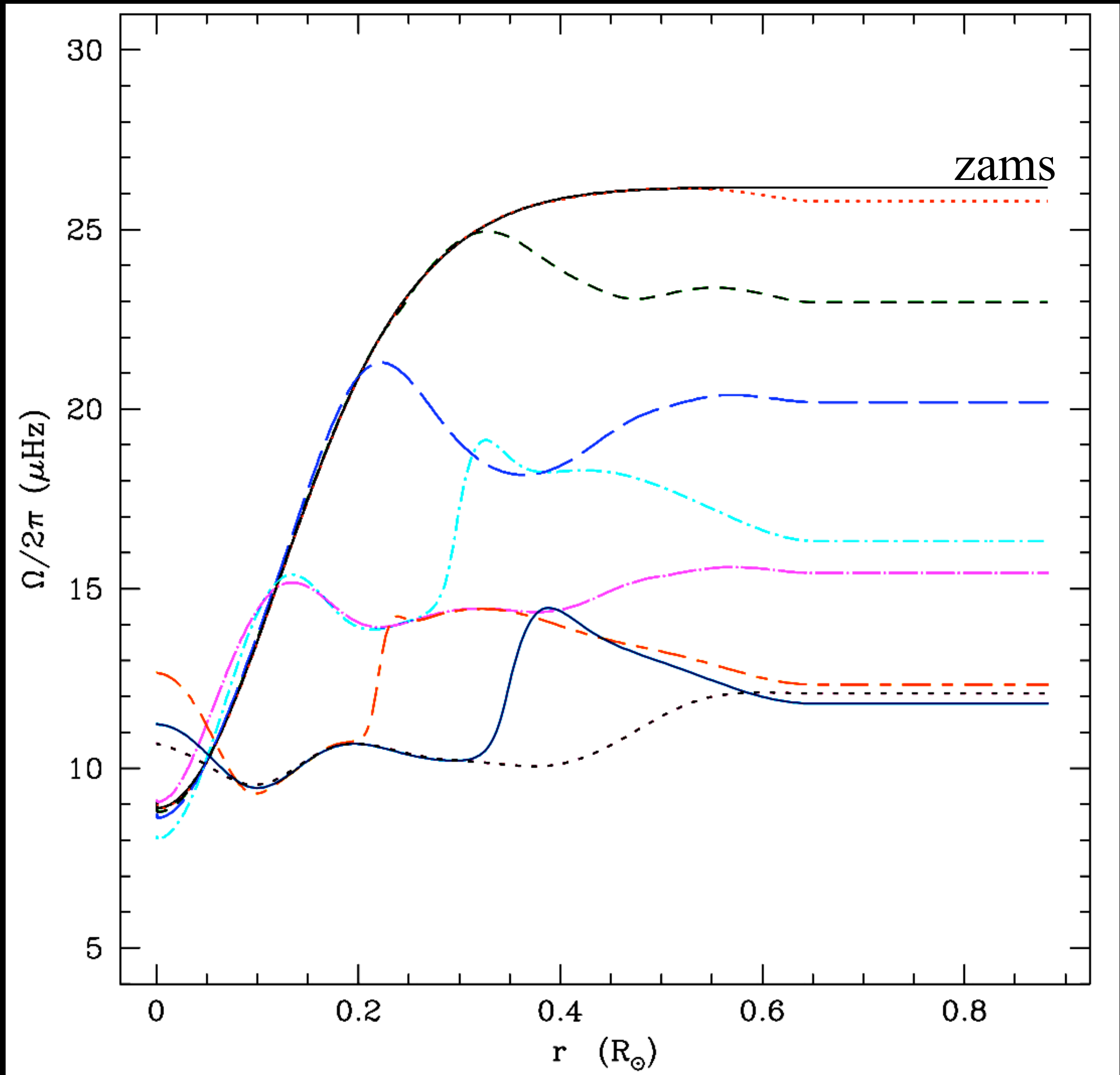

time

98, 100, 105, 110, 115, 120, 125, 130 Myr

Charbonnel, Decressin & Talon (in prep.)

Main sequence

$1M_\odot$
V_i = 20 km/sec
$Prot_i$ = 5 d
Vzams = 102 km/sec

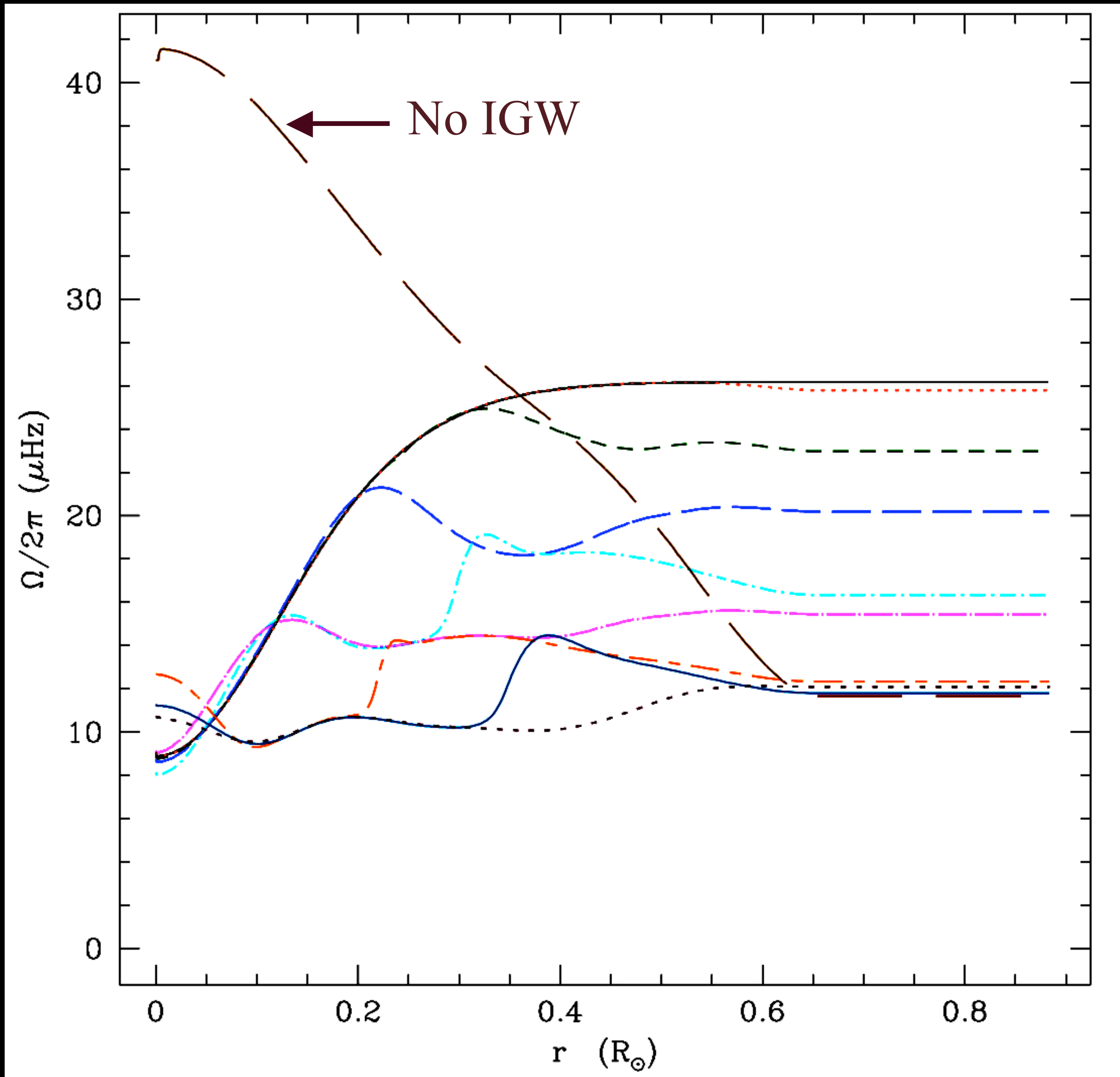

9.8e7, 1e8, 1.05e8, 1.1e8, 1.15e8, 1.2e8, 1.25e8, 1.3e8

Charbonnel, Decressin & Talon (in prep.)

Bridging the gap

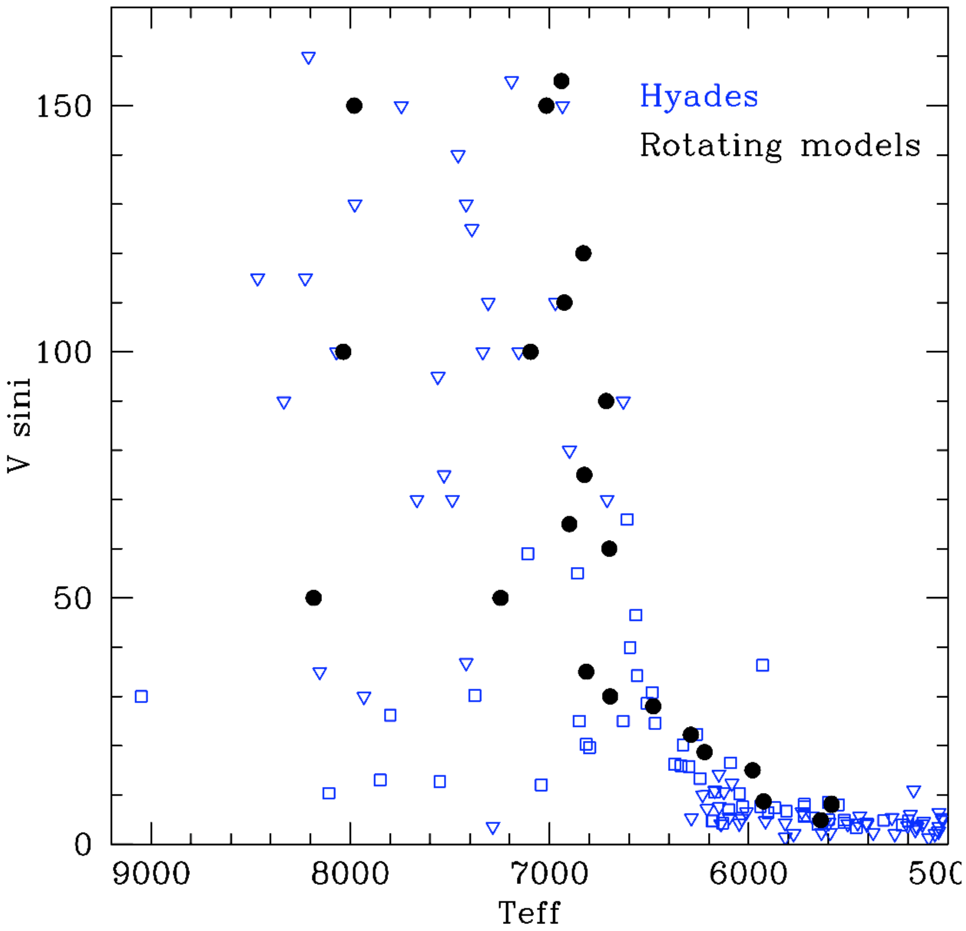

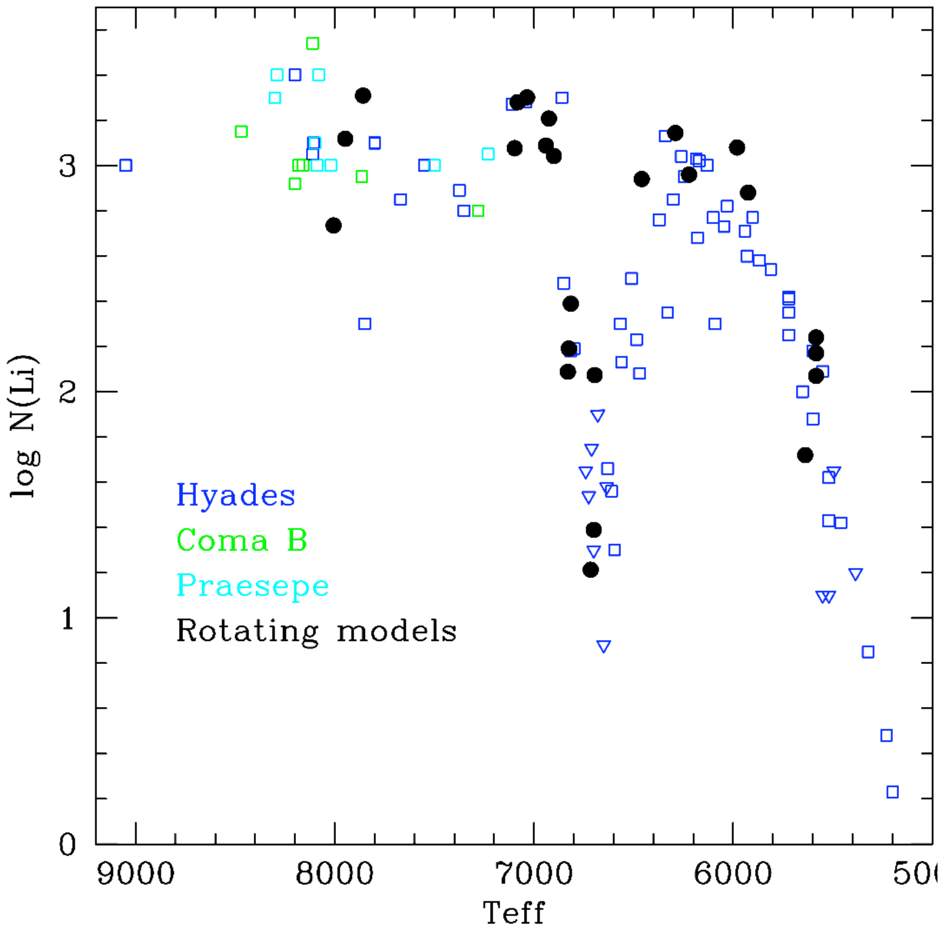

Charbonnel, Decressin & Talon (in prep.)

Transport of angular momentum dominated by
Circulation and turbulence in massive stars down to the Li dip
Internal gravity waves in low mass stars with deeper convective envelopes

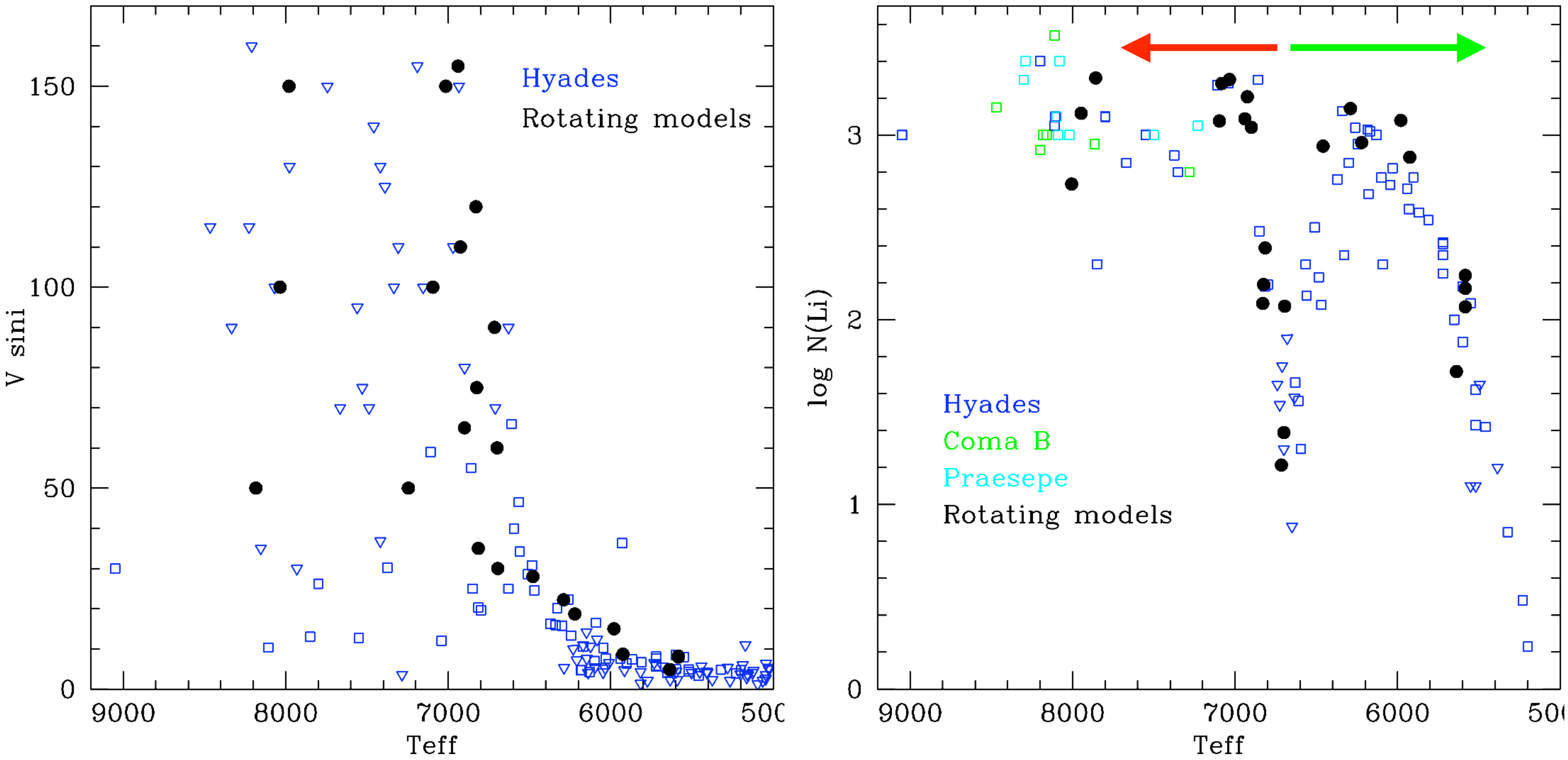

Charbonnel, Decressin & Talon (in prep.)

Pop II stars

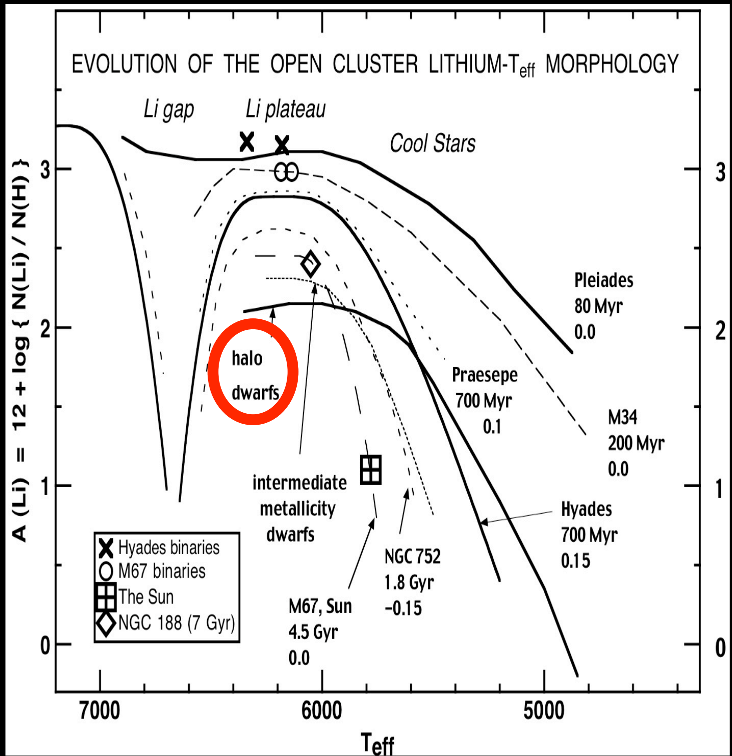

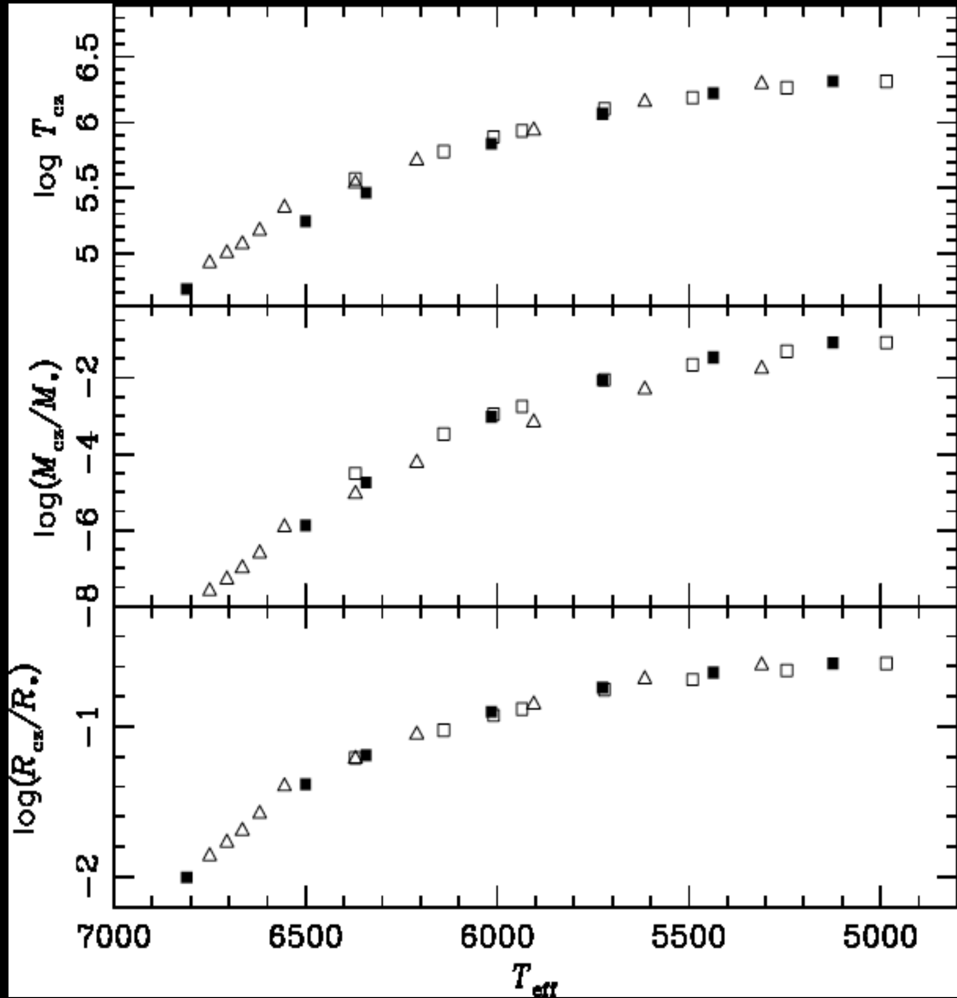

Open squares : Pop II stars ([Fe/H]=-2) on the zams
Black squares : Pop II stars ([Fe/H]=-2) at 10 Gyr
Open triangles : Pop I stars on the zams

Talon & Charbonnel (2004)

Pop II stars

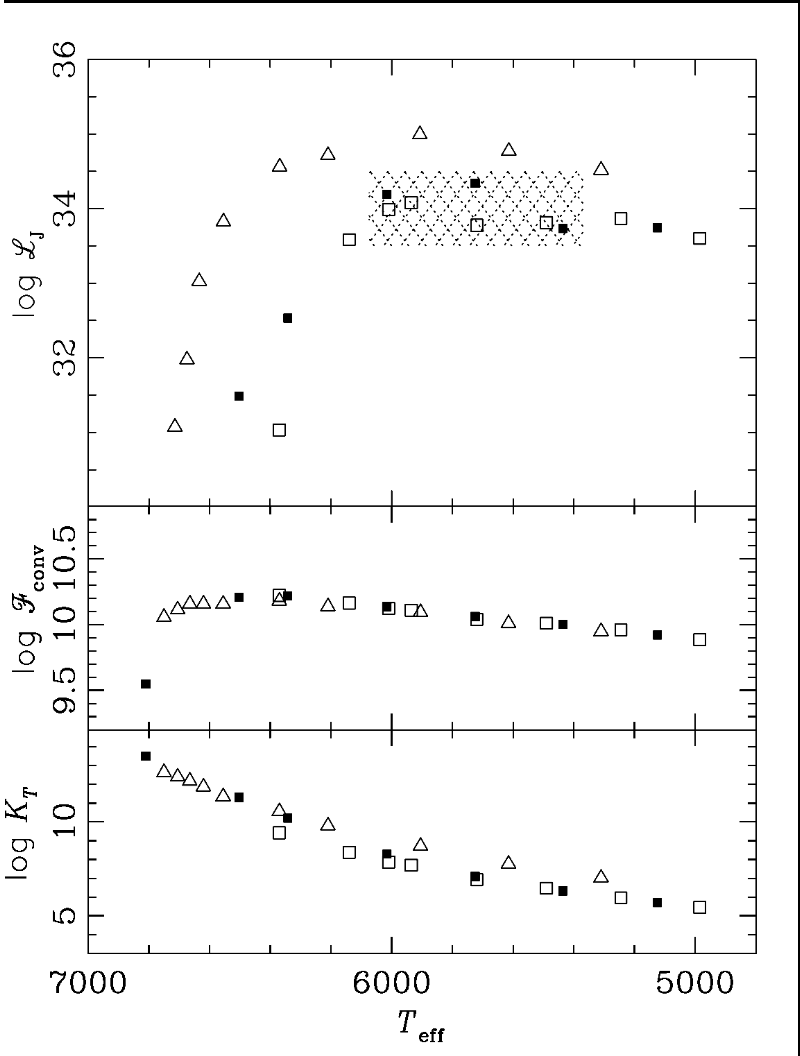

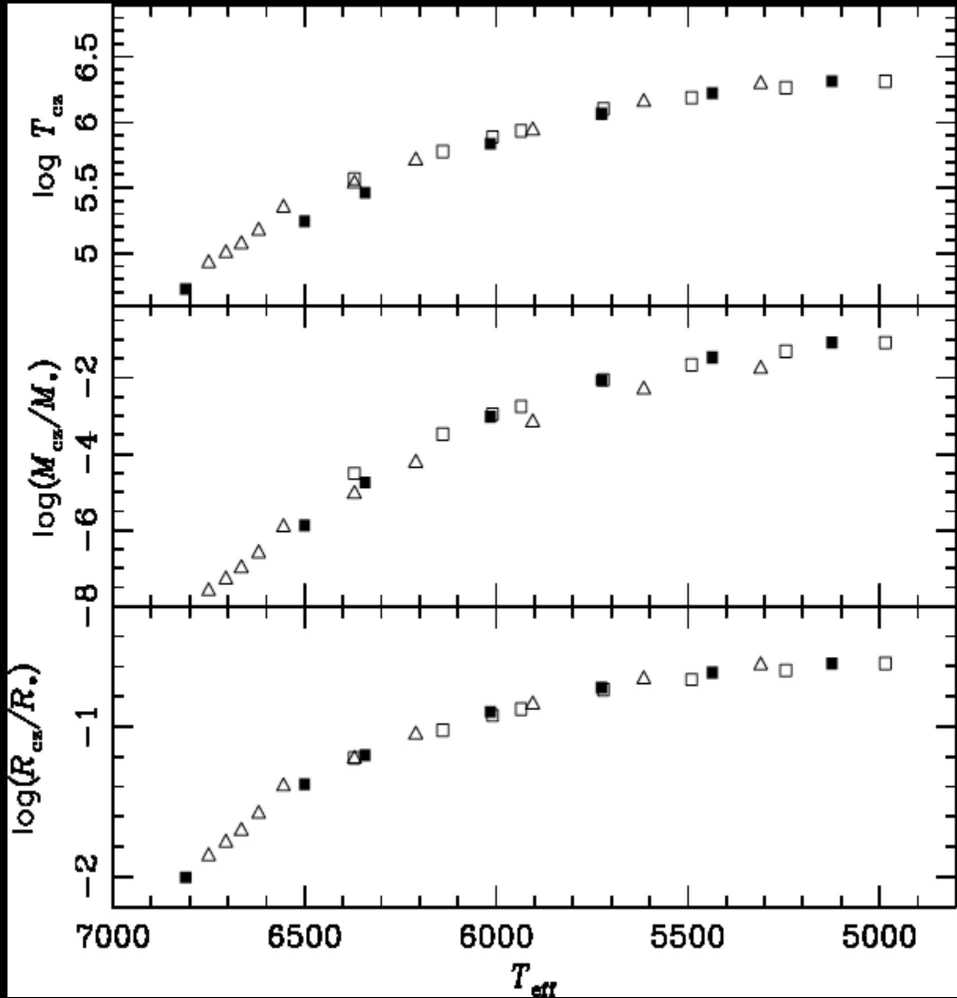

Open squares : Pop II stars ([Fe/H]=-2) on the zams
Black squares : Pop II stars ([Fe/H]=-2) at 10 Gyr
Open triangles : Pop I stars on the zams

Talon & Charbonnel (2004)

Pop II stars

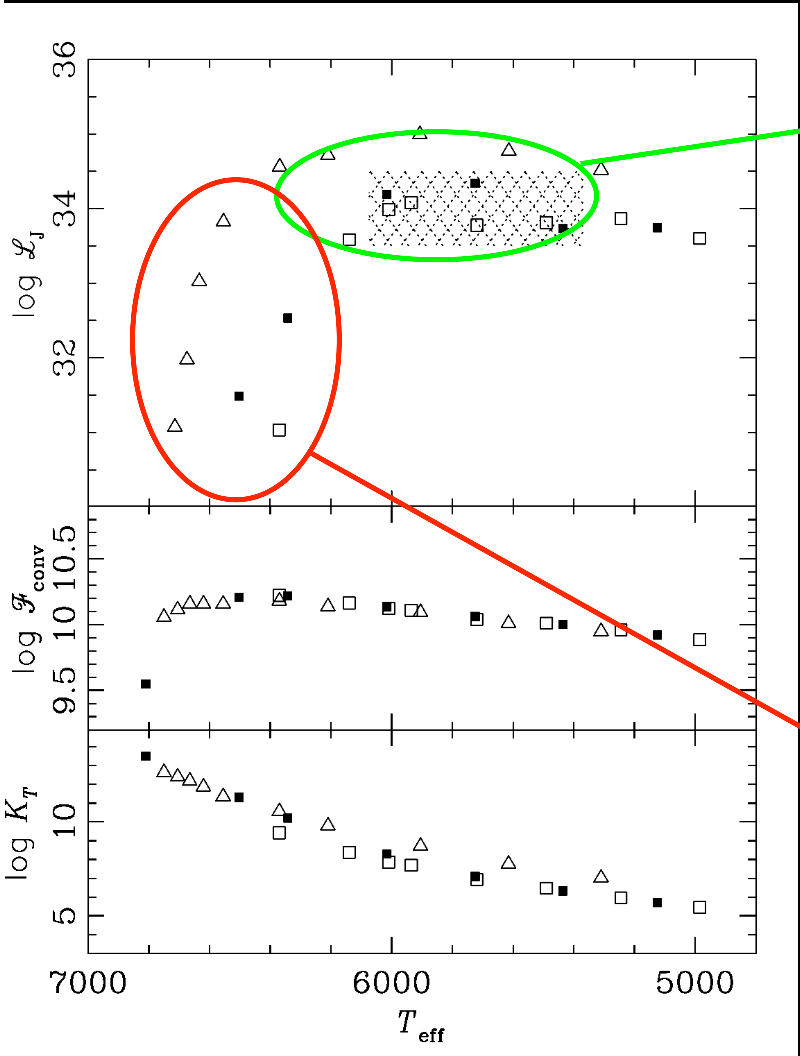

Dwarf stars lying on the Spite plateau
⇔IGWs dominate the transport of angular momentum
→ Solid body rotators
→ Decrease of the surface Li abundance but very little Li dispersion

Slightly more massive stars
→ Large internal differential rotation
→ More Li dispersion (Charbonnel & Primas 05)
→ High Vsin observed on the horizontal branch

Talon & Charbonnel (2004)

Pre-main sequence

0.7 $M_\odot$, [Fe/H]=-2
V_i = 10 km/sec
Vzams = 30 km/sec

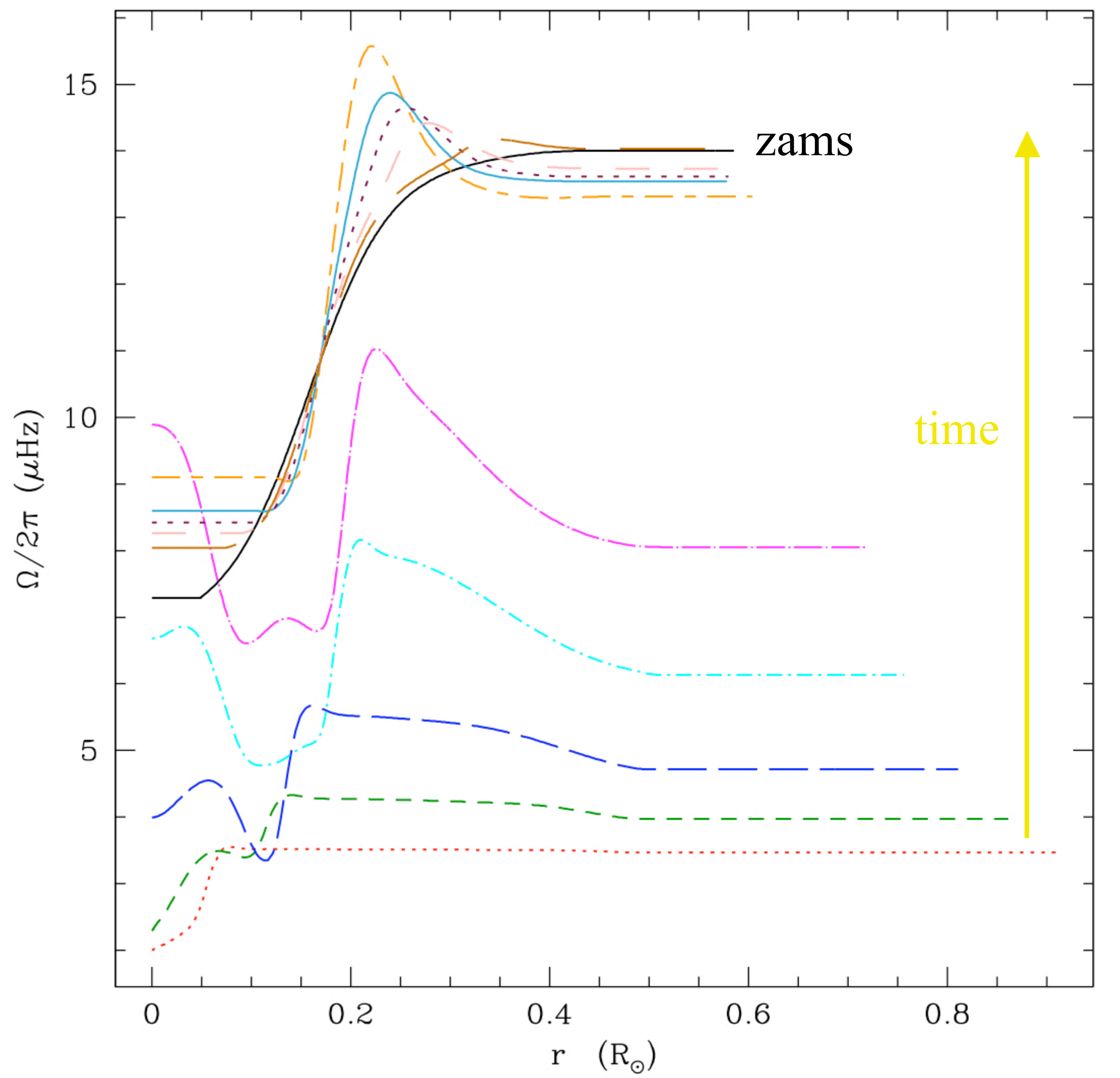

6.2, 8, 11, 16.5, 22, 36, 51, 654, 80, 98, 125, 159 Myrs

Charbonnel, Decressin & Talon (in prep.)

Main sequence

0.7 $M_\odot$, [Fe/H]=-2
V_i = 10 km/sec
Vzams = 30 km/sec

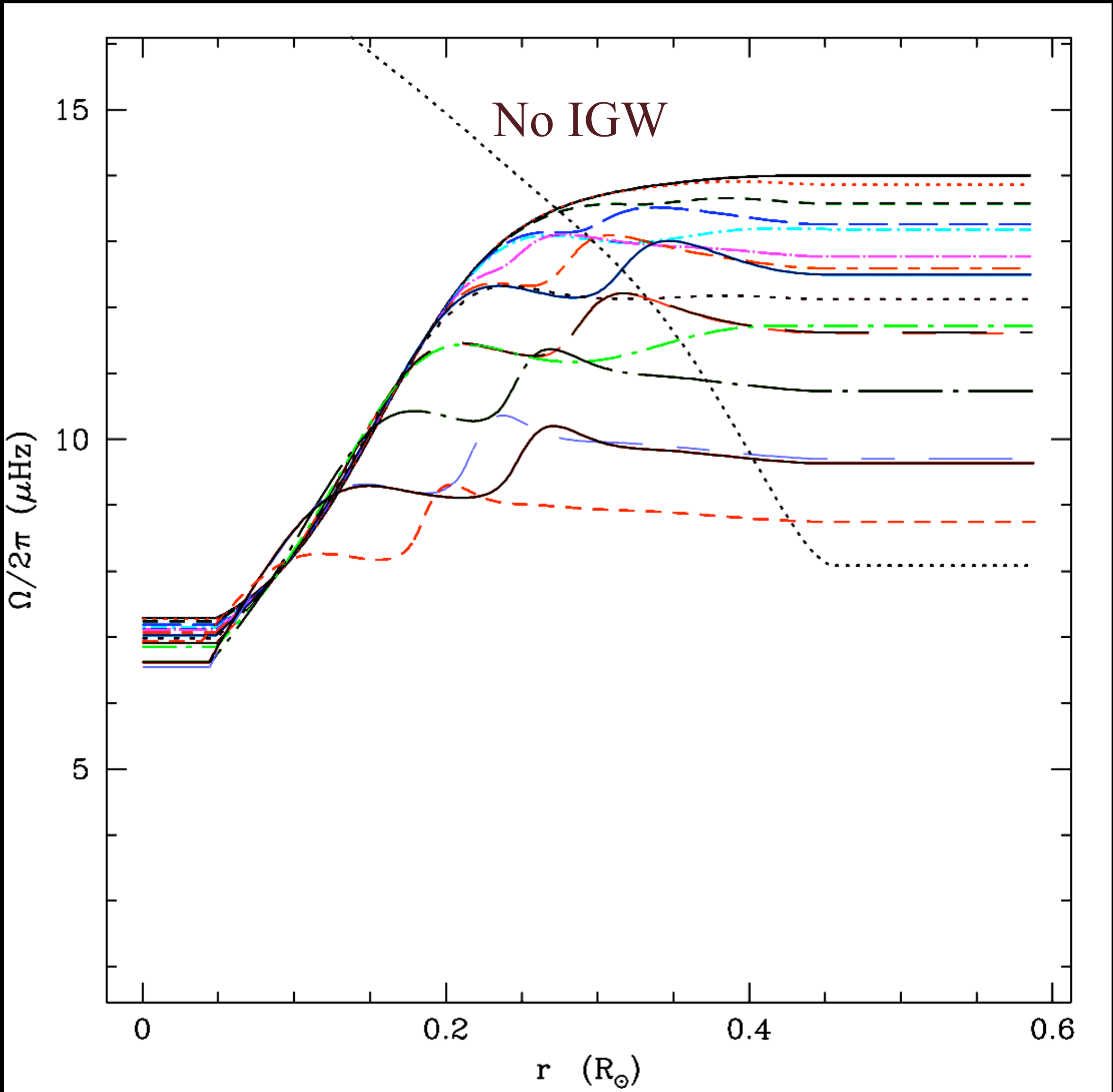

159, 161, 165, 170, 175, 180, 185, 190, 200, 216, 225, 250, 300, 308, 360 Myrs

Charbonnel, Decressin & Talon (in prep.)

Pop II stars at very low metallicity

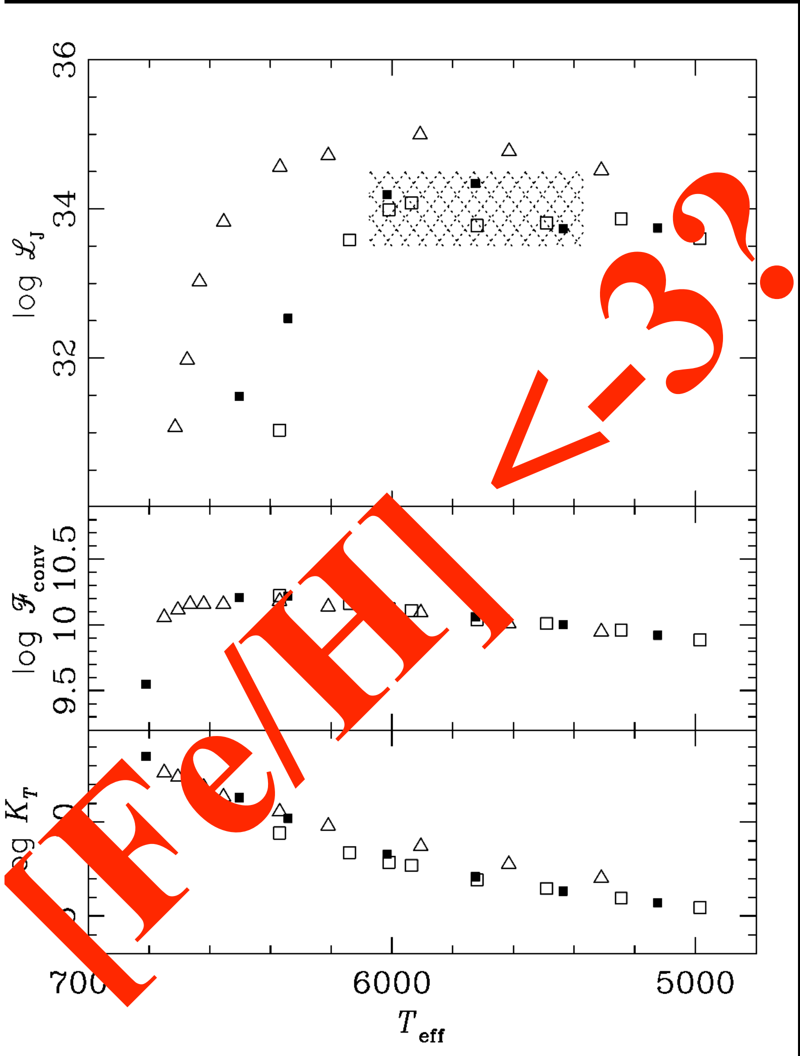

Dwarf stars lying on the Spite plateau
at low Z ([Fe/H] < -3)
⇔Do IGWs still dominate the transport of
angular momentum ?

→ If not, then they would behave like Pop I stars of the left side of the Li dip
i.e., Li depletion depends on angular momentum extraction
→ Li dispersion should then reflect dispersion in initial rotation velocity

Stay tuned!

Open squares : Pop II stars ([Fe/H]=-2) on the zams
Black squares : Pop II stars ([Fe/H]=-2) at 10 Gyr
Open triangles : Pop I stars on the zams

Talon & Charbonnel (2004)